Functional determinants of a small protein controlling a broadly conserved bacterial sensor kinase

Srujana S Yadavalli[2, 3]*, Ted Goh[4,5], Jeffrey N Carey[6], Gabriele Malengo[1,7], Sangeevan Vellappan[8], Bryce E Nickels[3], Victor Sourjik[1,7], Mark Goulian[2,9]* and Jing Yuan[1,7]*

[1]Max Planck Institute for Terrestrial Microbiology, 35043 Marburg, Germany
[2]Department of Biology, University of Pennsylvania, Philadelphia, Pennsylvania 19104, USA
[3]Department of Genetics and Waksman Institute of Microbiology, Rutgers University, Piscataway, NJ 08854, USA
[4]Department of Biology, Swarthmore College, Swarthmore, Pennsylvania 19081, USA
[5] Boston University School of Medicine, Boston, Massachusetts 02118, USA
[6]Biochemistry and Molecular Biophysics Graduate Group, Perelman School of Medicine, University of Pennsylvania, Philadelphia, Pennsylvania 19104, USA
[7]LOEWE Center for Synthetic Microbiology (SYNMIKRO), 35043 Marburg, Germany
[8]Molecular Biosciences Graduate Program, Rutgers University, Piscataway NJ 08854
[9]Department of Physics, University of Pennsylvania, Philadelphia, Pennsylvania 19104, USA

*Corresponding authors. J.Y.: jing.yuan@synmikro.mpi-marburg.mpg.de, S.S.Y.: sam.yadavalli@rutgers.edu, M.G.: goulian@sas.upenn.edu

Abstract

The PhoQ/PhoP two-component system plays a vital role in the regulation of Mg^{2+} homeostasis, resistance to acid and hyperosmotic stress, cationic antimicrobial peptides, and virulence in *Escherichia coli*, Salmonella and related bacteria. Previous studies have shown that MgrB, a 47 amino acid membrane protein that is part of the PhoQ/PhoP regulon, inhibits the histidine kinase PhoQ. MgrB is part of a negative feedback loop modulating this two-component system that prevents hyperactivation of PhoQ and may also provide an entry point for additional input signals for the PhoQ/PhoP pathway. To explore the mechanism of action of MgrB, we have analyzed the effects of point mutations, C-terminal truncations and transmembrane region swaps on MgrB activity. In contrast with two other known membrane protein regulators of histidine kinases in *E. coli,* we find that the MgrB TM region is necessary for PhoQ inhibition. Our results indicate that the TM region mediates interactions with PhoQ and that W20 is a key residue for PhoQ/MgrB complex formation. Additionally, mutations of the MgrB cytosolic region suggest that the two N-terminal lysines play an important role in regulating PhoQ activity. Alanine scanning mutagenesis of the periplasmic region of MgrB further indicates that, with the exception of a few highly conserved residues, most residues are not essential for MgrB's function as a PhoQ inhibitor. Our results indicate that the regulatory function of the small protein MgrB depends on distinct contributions from multiple residues spread across the protein. Interestingly, the TM region also appears to interact with other non-cognate histidine kinases in a bacterial two-hybrid assay, suggesting a potential route for evolving new small protein modulators of histidine kinases.

Introduction

Small proteins—proteins less than 50-amino acids long that are directly translated from small open reading frames—regulate a wide variety of cellular processes but, collectively, this class of proteins remains relatively understudied (reviewed in [1, 2]). For example, hundreds to thousands of small open reading frames have been reported in *Escherichia coli* [3-5], *Mycobacterium tuberculosis* [6] and human microbiomes [7]. A fraction of them have been confirmed with detections at the protein level [3-6] and the functions of most these

proteins are unknown. In bacteria and bacteriophages, small proteins can be classified into two groups: secreted and non-secreted [1]. The former are mainly involved in communication or competition among organisms, whereas the latter are localized in the cytoplasm or cell membrane and play a role in diverse aspects of cell physiology. In *E. coli*, the list of small proteins that have been identified and verified continues to grow with improvements in computational and experimental techniques [3, 4, 8]. Interestingly, nearly one third have been shown or are predicted to be in the cytoplasmic membrane, suggesting many may be involved in sensing environmental cues and mediating stress responses.

Bacteria thrive in a multitude of niches, often under challenging physicochemical conditions, and have therefore evolved stress response systems to monitor the environment and modulate their physiology accordingly. Many of these stress responses are controlled by two-component signaling systems, one of the primary modes of bacterial signal transduction [9]. The PhoQ/PhoP system in *E. coli*, Salmonella, and related Gram-negative bacteria is a well-studied example of a two-component system that is critical for virulence and facilitates adaptation to conditions of low Mg^{2+} or Ca^{2+}, low pH, osmotic upshifts and the presence of cationic antimicrobial peptides [10-14]. In response to input signal, the sensor histidine kinase PhoQ autophosphorylates and modulates the phosphorylation state of the response regulator PhoP, which functions as a transcription factor [10, 15]. At least three small proteins are regulated by PhoP: the 31-amino acid membrane protein MgtS is induced under magnesium limitation in *E. coli* and inhibits degradation of the magnesium transporter MgtA [16]; the 30-amino acid protein MgtR promotes the degradation of the virulence factor MgtC by the FtsH protease in *Salmonella enterica* serovar Typhimurium [17]; and the 47-amino acid protein MgrB directly inhibits PhoQ kinase activity, thereby mediating a negative feedback loop [18, 19]. All of these small proteins are membrane-localized, regulate proteins expressed in the PhoP regulon, and modify cell responses to the environment.

MgrB orthologs are found in numerous Enterobacteriaceae, and PhoQ inhibition has been demonstrated explicitly for a few distinct genera. The physiological importance of this inhibition and the associated negative feedback loop remain poorly understood. MgrB could serve as a point of control for additional input signals that modulate PhoQ. For example, MgrB activity is affected by the redox state of the periplasm via the protein's two conserved periplasmic cysteines [20]. MgrB is not essential and appears to mainly act in a regulatory role, however it can have a significant impact on bacterial physiology. In *E. coli*, recent work has shown that strong stimulation of the PhoQ/PhoP system hinders cell division [21]. Cells grown in low levels of Mg^{2+} in the absence of MgrB form filaments due to strong activation of PhoQ in this condition. MgrB-mediated feedback inhibition thus appears to be important to appropriately limit PhoQ activity and prevent hyperactivation of the system. In at least some contexts, loss of *mgrB* can also confer a fitness advantage: mutation of *mgrB* has emerged as one of the primary mechanisms of acquired resistance to the last resort antibiotic colistin in clinical isolates of *Klebsiella pneumoniae* [22-25].

In addition to MgrB, the PhoQ histidine kinase is modulated by another membrane protein, SafA [26], which is present exclusively in *E. coli*, and acts as a connector between the EvgS/EvgA and PhoQ/PhoP two-component systems. Stimulation of EvgS by low pH upregulates SafA expression [27], which activates PhoQ kinase activity and leads to increased acid resistance. In at least some *E. coli* isolates, this connection is required for PhoQ activation in response to acid stress [28, 29]. Another example of a connector protein that modulates the activity of a histidine kinase is MzrA [30], which links the CpxA/CpxR and EnvZ/OmpR two-component systems. Although not as small as MgrB, both SafA and MzrA are relatively small for membrane proteins (65 and 127 amino acids, respectively) and, like MgrB, are bitopic with their N-termini in the cytoplasm.

MgrB acts by inhibiting PhoQ kinase activity [19], however, the mechanism by which this small protein inhibits a protein that is roughly ten times larger than itself, and the sequence

determinants responsible for this action are largely unknown. In this work, we show that the transmembrane (TM) region of MgrB is required for the protein to form a complex with its target kinase PhoQ, in contrast with SafA and MzrA, which do not require their TM regions for their activity [31, 32]. Using site-directed mutagenesis combined with MgrB functional assays and *in vivo* Förster resonance energy transfer (FRET), we identified W20 in the MgrB TM region to be crucial for MgrB/PhoQ complex formation. Additionally, we identified 11 residues across different regions of MgrB that are important for its inhibitory function. Among these residues, two lysines in the cytoplasmic region likely act through their charged side chains to regulate PhoQ HAMP conformation, although they do not appear to affect MgrB/PhoQ complex formation. Surprisingly, a large number of amino acids in the small periplasmic region of MgrB can be replaced with alanine with only minor effects on protein function. Together our findings suggest that PhoQ inhibition by MgrB depends on coordinated interactions from amino acid residues spanning different regions of the protein. We also uncovered interactions of MgrB with other histidine kinases in bacterial two-hybrid assays, which may provide a starting point for evolving novel small membrane proteins that modulate other histidine kinases.

Results

Sequence analysis of MgrB

MgrB was shown to be a membrane-localized small protein with N-terminal-in and C-terminal-out topology [18]. To predict the transmembrane (TM) region in MgrB, we used eight algorithms (PHDHTM, DAS-TMFILTER, SCAMPI, TMHMM, TMpred, TMMTOP, PRED-TMR and MEMSAT) to analyze the entire amino acid sequence (Fig 1). The predictions were fairly convergent on the TM cytoplasm/membrane boundary, which was located at W6 or V7. In contrast, the predictions of the membrane/periplasm boundary were quite different among these programs, ranging from F24 to M27. In this manuscript, we use W6 to F24 as the predicted transmembrane region of MgrB.

To gain insight on potential functionally important residues in MgrB, we aligned over 100 bacterial MgrB sequences obtained from KEGG protein BLAST using *E. coli* MgrB as query (Fig 1 and supplementary file 1). As indicated in the sequence logo of the alignment, the amino acids were fairly conserved in the cytosolic and periplasmic regions. This high degree of conservation might originate from limitations in the diversity of MgrB sequences currently available in databases or suggest the functional importance of each conserved amino acid in these regions. In contrast, more variations and insertion of one amino acid were shown in the predicted TM region. Interestingly, two amino acids with polar side chains (C16 and Q22) and two tryptophans (W6 and W20) in the TM region are highly conserved, suggesting a functional importance.

MgrB TM and periplasmic regions are necessary but not sufficient for MgrB function

As a first step towards understanding how MgrB inhibits PhoQ at a structural level, we looked at the role of the protein's TM and periplasmic regions. To test the functional role of the MgrB TM region, we swapped the predicted MgrB TM region with either (i) a 20-amino acid TM from the *E. coli* maltose transporter MalF or (ii) a 21-amino acid variant of human glycophorin A (GpA) TM [33] (Fig 2A). The MgrB variants described in this section are derivatives of a functional N-terminally GFP tagged MgrB (GFP-MgrB) [18]. Both MgrB variants with swapped TM regions localized to the cell membrane (S1 Fig) and their expression levels were comparable to that of wild type (S2 Fig). TM swapping experiments of two previously studied histidine kinase regulators–SafA and MzrA—indicate that the transmembrane sequence is dispensable for their function [31, 32]. Indeed, our control experiments in which we replaced the TM sequences of SafA and MzrA with that of GpA

confirmed these results (S3 Fig). Thus, for SafA and MzrA, the TM region appears to primarily act as an anchor to direct the regulatory domain of these proteins to the membrane. We monitored the effect of MgrB and its TM swap variants on PhoQ activity using a PhoQ/PhoP-regulated transcriptional reporter (P_{mgtA}-*lacZ*) (Fig 2A). Control cells expressing no MgrB had a high level of β-galactosidase (β-gal) activity, indicating uninhibited PhoQ, whereas cells expressing WT MgrB had minimal β-gal activity, indicating PhoQ inhibition by WT MgrB as expected. In contrast to the inhibitory function of the WT MgrB, both MgrB TM swap variants (MgrB-MalF TM and MgrB-GpA TM) showed high β-gal activities that were about 80% of the activity of no-MgrB control, indicating that they are unable to inhibit PhoQ efficiently. These results suggest that the MgrB TM region not only functions as a membrane anchor but also has additional properties that are critical for MgrB to inhibit PhoQ.

As swapping the TM sequence in MgrB severely affected its activity, we tested whether an MgrB mutant lacking the periplasmic region inhibits PhoQ. This variant—MgrB-24, in which N25 is replaced with a stop codon—showed proper membrane localization (S1 Fig), but could not repress reporter gene expression (Fig 2B), indicating that this truncated variant composed of the MgrB TM and short N-terminal cytoplasmic regions is not functional. To assess the minimum length of MgrB needed for efficient repression of PhoQ/PhoP-regulated reporter gene expression, we tested other C-terminal truncations of MgrB: MgrB-29, MgrB-34, MgrB-39, MgrB-44, corresponding to replacing the codons for Q30, F35, A40 and I45 with a stop codon, respectively. These mutants displayed similar membrane localization to that of WT MgrB (S1 Fig). Of these four truncations, MgrB-29 and -34 did not show any detectable repression, MgrB-39 showed slight repression, and MgrB-44, which lacks only the last two residues, showed the strongest repression, although last variant was still compromised in activity compared with WT (Fig 2B). Evidently, amino acid interactions in both the TM and the periplasmic region of MgrB influence the protein's ability to inhibit PhoQ.

Previous work suggested that the periplasmic region of MgrB is required for PhoQ inhibition [18]. Since the TM swaps described above change the TM helix length, their loss of activity could be due to a change in the helical phase at the C-terminus of the TM helix creating different orientations of the periplasmic region. It is therefore possible that the periplasmic region of MgrB alone could inhibit PhoQ, while the TM helix only ensures its correct orientation. Indeed, the chemically synthesized periplasmic region of SafA ($SafA^{peri}$) was previously shown to be sufficient for PhoQ activation when added exogenously [34]. Therefore, we tested whether the MgrB periplasmic region ($MgrB^{peri}$) could function similarly to full-length MgrB (Fig 2C) by adding $MgrB^{peri}$ to an *E. coli* culture. To enable the $MgrB^{peri}$ peptide to access the periplasm, we used an *imp-4213* strain, which has increased outer membrane permeability [35]. We monitored PhoQ activity with a GFP reporter fused to the promoter region of a PhoQ/PhoP regulated gene (pUA66 P_{mgtLA}-*gfp*) in the presence or absence of chemically synthesized $MgrB^{peri}$. The positive control, chemically synthesized $SafA^{peri}$, enhanced PhoQ activity significantly, consistent with the previous report [34]. In contrast, $MgrB^{peri}$ did not show any inhibitory effect on PhoQ activity in the concentration range that we tested, though DMSO the solvent for $MgrB^{peri}$ peptide showed a slight inhibition of *gfp* reporter expression. As $MgrB^{peri}$ is short and likely capable of sampling different conformations, our results suggest that, unlike SafA, the MgrB periplasmic region alone is not sufficient to inhibit PhoQ. Taken together, the above results indicate that both the MgrB TM and periplasmic regions are required but not sufficient to inhibit PhoQ.

MgrB lacking its periplasmic region is capable of physical interaction with PhoQ

Although MgrB-24 (N-terminal region+TM region) does not inhibit PhoQ, it could still play a role in establishing physical contact with PhoQ. To explore this possibility, we used a

bacterial two-hybrid (BACTH) system based on split adenylyl cyclase [36, 37]. In the assay, reconstitution of the T18 and T25 fragments restores the activity of adenylate cyclase (CyaA), which leads to an increase in cAMP levels. This increased cAMP in turn enables efficient induction of the genes required for maltose catabolism, resulting in pink colonies on maltose MacConkey plates. To assay interactions of MgrB lacking its periplasmic region with PhoQ, we prepared N-terminal fusions of MgrB-24 and PhoQ to T18 and T25 fragments, respectively. As controls, we tested interactions between MgrB–PhoQ, MgrB–*Vc*ToxR (*Vibrio cholerae* inner membrane protein ToxR) as well as MgrB–T25 fragment alone. Spot assays of cells expressing T18-MgrB-24 and T25-PhoQ produced a dark pink color after 48 h at 30 °C, whereas cells expressing T18-MgrB-24 and the T25 fragment alone were colorless (Fig 2D). Spots of cells expressing T18-MgrB-24 and either T25-MgrB or T25-MgrB-24 were also pink. Control cells expressing T18-MgrB and either T25-PhoQ or T25-MgrB formed dark pink spots, showing an interaction of MgrB with PhoQ and possibly with itself, consistent with previous work [18], whereas control cells expressing either T18-MgrB or T18-MgrB-24 with either T25-*Vc*ToxR or T25 fragment alone remained colorless. Taken together, these results suggest that the MgrB N-terminus+TM region interacts with PhoQ and may also interact with itself to facilitate formation of a multimeric complex.

A small number of functionally important residues are spread across different regions of MgrB

To explore the relative importance of different residues in MgrB, we made alanine substitutions and analyzed their effects on PhoQ inhibition. Interestingly, a majority of the substitutions in MgrB did not affect PhoQ/PhoP reporter gene expression, but 11 substitutions spread across different regions showed significant activation of the reporter gene (Figs 5, S4, and S5), indicating impaired MgrB activity. We confirmed that each of these 11 MgrB variants was localized to the membrane with expression levels that were comparable to that of wild-type MgrB (S1 and S2 Fig). Below we discuss these 11 MgrB variants in more detail.

a. Two lysines in the MgrB cytosolic region regulate PhoQ activity.

In the short N-terminal cytosolic region of MgrB (M1 to R5), we made alanine substitutions at each position except the first methionine. Here, we used the PhoQ/PhoP regulated GFP reporter (pUA66 P_{mgtLA}-*gfp*) to monitor the activities of MgrB variants. Control cells having no MgrB expression showed a high intensity of GFP fluorescence, while cells expressing wild-type MgrB had much lower reporter fluorescence (Fig 3A). The K2A and K3A substitutions displayed the most effect on *gfp* reporter expression, with fluorescence comparable to the no-MgrB control (Fig 3A). F4A and R5A had about 50% and 80% activity, respectively. K2A and K3A, however, only retained about 20% activity (Fig 3A, see Materials and Methods for the definition of normalized activity).

To further investigate whether this loss of activity might be caused by deficient protein interactions, we used *in vivo* acceptor photobleaching FRET [38] to test complex formation between these two MgrB variants and PhoQ. In this assay, MgrB variants and PhoQ were tagged with a red fluorescent protein (mCherry) and a green fluorescent protein (mNeonGreen) respectively and co-expressed in an *E. coli* Δ*phoQ* Δ*mgrB* strain. Complex formation between tagged proteins typically results in close proximity and consequently energy transfer between the donor mNeonGreen and the acceptor mCherry, leading to quenching of the mNeonGreen fluorescence. The latter can be detected as an increase in the mNeonGreen fluorescence upon photobleaching of mCherry that abolishes FRET (see Materials and Methods). The apparent FRET efficiency could be defined as the resulting increase in the donor fluorescence divided by its fluorescence after bleaching [39]. While apparent FRET efficiencies may vary depending on the optical set-up, for intra-molecular mNeonGreen-mCherry tandem constructs the reported values are in the range of 15-20%

[40]. We observed about 7.0% FRET efficiency for PhoQ-mNeonGreen/mCherry-MgrB WT, whereas the negative control, PhoQ-mNeonGreen/mCherry, showed only about 1.5% FRET efficiency. Interestingly, K2A and K3A mutants showed similar FRET efficiency as MgrB WT (Fig 3C), suggesting that substitutions at these two positions do not significantly affect the MgrB/PhoQ complex formation. Therefore, K2 and K3 may be instead directly involved in regulating PhoQ conformation and promoting a kinase-inactive state of the enzyme.

We speculated that MgrB might regulate PhoQ conformation through the positively charged side chains of K2 and K3. To test this hypothesis, we mutated K2 or K3 to a negatively charged amino acid. Mutating K2 or K3 individually to aspartate only slightly reduced MgrB function (S4 Fig A and B). Furthermore, when we substituted these two lysines individually with 19 other amino acids, many of the mutants retained more than 50% activity (S4 Fig A and B). Thus, neither K2 nor K3 alone is essential for MgrB function. We then tested the effect of replacing both K2 and K3 with aspartate. MgrB K2DK3D localized to the cell membrane similarly to wild-type MgrB (S1 Fig) but with some reduced expression (S2 Fig). At this expression level, the K2DK3D mutant appeared to be a mild PhoQ activator rather than an inhibitor and showed a 20% higher reporter activity compared to the no MgrB control (Fig 3B). Increasing MgrB K2DK3D expression, either by doubling the amount of arabinose inducer or by using a stronger promoter (*trc* promter), produced a small level of inhibition that was much less than the level of inhibition of wild-type MgrB (S4 Fig C and D). Double mutants, in which the lysines were replaced with either of the positively charged amino acids histidine or arginine (K2HK3H and K2RK3R), on the other hand, retained about 60% inhibitory activity (Fig 3B). FRET analyses also showed that MgrB K2DK3D had a FRET efficiency comparable to that of wild type (Fig 3C), indicating that this MgrB variant forms complexes with PhoQ. Taken together, our results suggest that the two lysines in the MgrB cytosolic region regulate PhoQ function through their positively charged side chains without contributing to PhoQ/MgrB complex formation in *E. coli*. We interpret the fact that single amino acid substitutions of K2 or K3 to uncharged residues has little effect on activity as indicating that the remaining lysine is sufficient to mediate the required interaction. We also note that the K3R substitution was inactive (S4 Fig B), which suggests that it is not only the charge of the lysine sidechains that are important for MgrB activity.

b. The TM helix is involved in PhoQ/MgrB complex formation through W20.

Given that the MgrB TM sequence is necessary for its function, we wanted to further identify specific residues that might contribute to PhoQ inhibition. Polar amino acids such as N and Q can facilitate TM domain interactions by forming stable hydrogen bonds [41]. Aromatic residues are known to preferentially occur in the lipid-water interface regions [42, 43] and could be important for membrane anchoring as well as surface interactions. An MgrB sequence alignment identified four polar or aromatic residues in the transmembrane region that are highly conserved: W6, C16, W20 and Q22. Based on these considerations, we mutated the four highly conserved residues and F24 individually to alanine. The W6A and C16A substitutions did not affect MgrB function (S5 Fig and Fig 4A); the result for C16A is consistent with previous observations [20]. The F24A substitutions displayed modest effect on reporter gene expression (~8-fold higher β-gal activity compared to WT MgrB) and the change in activity for the Q22A mutant was not statistically significant (Fig 4A). The W20A substitution, on the other hand, greatly affected MgrB function, with β-gal reporter activity that was ~30-fold higher than that of WT MgrB (Fig 4A). These results were also reproduced with the GFP reporter system and untagged MgrB (S5 Fig), except that the Q22A showed significant activity loss (~70%) in this case. Collectively, the results from both approaches indicate that W20, F24 and possibly Q22 in the TM region are functionally important.

Our bacterial two-hybrid data suggest that the MgrB TM region plays a role in establishing physical contact with PhoQ. To pinpoint the essential residues in MgrB TM region that are responsible for MgrB/PhoQ complex formation, we performed FRET analyses on MgrB TM

328 point mutants (Fig 4B). Compared to wild-type MgrB, which had 7.0% FRET efficiency,
329 Q22A and F24A showed slightly reduced FRET efficiency, 5.7% and 5.2%, respectively.
330 W20A, on the other hand, produced a much greater change, with FRET efficiency reduced
331 to 2.4%, which was comparable to the negative control. These results indicate that W20 in
332 the TM region is a key residue for MgrB/PhoQ complex formation.
333
334 *c. The periplasmic region has six functionally important residues.*
335
336 In the periplasmic region, mutants C28A and C39A showed the highest effects (80-90 fold
337 higher β-gal activity than WT MgrB), consistent with previous data indicating that these
338 cysteines are important for MgrB activity [20]. In addition, mutants G37A, D31A, F34A and
339 W47A displayed a significant increase in reporter gene expression – approximately 30-, 8-,
340 10-, and 10-fold relative to WT MgrB, respectively (Fig 5). These results were also
341 reproduced with GFP reporter system and untagged MgrB constructs (S5 Fig). The fact that
342 mutating residues C28, G37 and C39 showed the strongest effect on the reporter activity
343 suggests that these residues are likely important for structural stability of the MgrB
344 periplasmic region.
345
346 **A charged residue in the PhoQ TM2 – HAMP junction is involved in MgrB inhibition**
347
348 Our results suggest that the two N-terminal lysines in MgrB regulate PhoQ activity through
349 their charged side chains. To further explore which PhoQ residue(s) in PhoQ interact with
350 these lysines, we screened for PhoQ mutants for which MgrB K2DK3D showed increased
351 inhibitory activity. Based on the MgrB and PhoQ topologies, we hypothesized that K2 and K3
352 of MgrB interact with residues in the PhoQ TM2-HAMP region (Fig 6A). We therefore
353 mutated this region of PhoQ by error-prone PCR and screened for PhoQ mutants that have
354 reduced activity in the presence of MgrB K2DK3D. About 100 colonies with decreased green
355 fluorescent reporter protein were selected and the *phoQ* genes were sequenced. Mutants
356 with missense mutations are highlighted in the supplementary file (PhoQ_RM_screening).
357 Most of the missense mutations were clustered in/near TM2-HAMP junction and the second
358 helix of HAMP domain. We focused on the former, as residues in this region are more likely
359 to be close enough to interact with the lysines in MgrB. Among them, R219 (labeled in Fig
360 6A), which was the most frequent among identified mutations, appears to be the most
361 promising residue.
362
363 We therefore mutated PhoQ R219 to negatively charged amino acids (D and E) as well as
364 the amino acids with amide side chains (N and Q). Compared to wild-type PhoQ, R219D has
365 reduced activity (about 70% of WT), while the other three mutants (R219E, R219N and
366 R219Q) have activities that are either similar to or slightly greater than that of wild type (Fig
367 6B). Next, we tested the activity of these PhoQ mutants in the presence of MgrB K2DK3D.
368 Compared to wild-type PhoQ, R219D and R219E are indeed repressed further by MgrB
369 K2DK3D (Fig 6C), suggesting that reversing the side chain charge of PhoQ R219
370 compensates the effect of the charge inversion of MgrB N-terminal lysines. The inhibition of
371 PhoQ R219N and R219Q by MgrB K2DK3D, on the other hand, was comparable to the
372 inhibition of wild-type PhoQ, indicating that charge but not hydrogen bonding is important for
373 interactions of R219D and R219E with MgrB K2DK3D. We also found that wild-type MgrB
374 inhibited all four PhoQ R219 mutants to a similar extent as the inhibition of wild-type PhoQ
375 (Fig 6D), suggesting the existence of other factors involved in PhoQ inhibition by wild-type
376 MgrB.
377
378 **Inhibition of *E. coli* PhoQ by MgrB orthologs**
379
380 MgrB orthologs have previously been identified in several enterobacterial species [18]. To
381 examine the activities of these MgrB natural variants on *E. coli* PhoQ, we expressed MgrB
382 from *Klebsiella pneumoniae*, *Yesinia pestis*, *Photorhabdus laumondii*, *Proteus penneri*,

Providencia stuartii, *Serratia sp.MYb239*, *Enterobacter ludwigii* and *Salmonella enterica serovar typhimurium* in *E. coli* K-12 MG1655. All orthologs except one (MgrB-*E. ludwigii*) localized to the membrane (S1 Fig F). MgrB-*E. ludwigii*, which is missing the positively charged residues (K2, K3) in its N-terminus showed defective localization, suggesting the lack of a signal peptide. We found that most of the orthologs expressed at levels comparable to that of *E. coli* MgrB, but the ortholog from *E. ludwigii* expressed quite poorly in *E. coli* (~5-fold lower than *E. coli* MgrB see Fig 7). We then measured reporter gene expression for PhoP-regulated transcription as a function of activity of each MgrB ortholog (Fig 7). Unsurprisingly, *E. ludwigii* showed high reporter gene expression, indicating low PhoQ inhibition. MgrB from *K. pneumoniae, S. sp.MYb239,* and *S. typhimurium* showed small but significant increases in reporter activity (~4-fold, 2.5-fold, and 2-fold, respectively). Interestingly, *Y. pestis*, *P. penneri* and *P.stuartii* MgrB produced reporter activities that were significantly lower than that of *E. coli* MgrB, suggesting that they repress *E. coli* PhoQ more strongly than does *E. coli* MgrB.

MgrB interaction with non-cognate histidine kinases

To test if MgrB is capable of physically interacting with histidine kinases other than PhoQ, we made constructs of *E. coli* EnvZ, AtoS, CpxA, and PhoR fused to the T25 fragment of adenylyl cyclase and performed BACTH analysis by spot assays as well as by measuring β-gal activities of liquid cultures. Intriguingly, cells expressing T18-MgrB and either T25-AtoS, -EnvZ, or -PhoR showed a high level of activity, although less than the β-gal activity of cells expressing T18-MgrB and T25-PhoQ (Fig 8). Cells expressing T18-MgrB and T25-CpxA, on the other hand, displayed a level of β-gal activity only marginally higher than that of the negative controls. These results suggest that MgrB is capable of physically interacting with EnvZ, AtoS, and PhoR, at least in the context of the bacterial two-hybrid assay. To test whether MgrB affects the activity of these histidine kinases, we measured gene expression from promoters regulated by these histidine kinases, in the presence or absence of plasmid driven MgrB expression. However, we did not see any effect of MgrB on gene expression controlled by any of these histidine kinases (data not shown). We also tested several other histidine kinases: ArcB, BaeS, BasS, CpxA, CusS, EvgS, NtrB, RstB and TorS (S6 Fig). None of them showed interactions with MgrB that were comparable to that of PhoQ.

Discussion

In this study, we have explored the regions of the small protein MgrB that are important for its activity as an inhibitor of the PhoQ sensor kinase. Using a combination of biochemical and biophysical approaches, we identified 11 amino acids in MgrB that, at least in the context of alanine substitution, are important for the protein's inhibition of PhoQ . These functionally important residues are spread across different regions of the molecule, consistent with our observation that TM replacement or periplasmic region truncation leads to a loss of MgrB function. The fact that the MgrB TM sequence is required for the protein's activity distinguishes MgrB from at least two other bitopic membrane proteins that regulate histidine kinases (SafA and MzrA); the TM domains of SafA and MzrA apparently serve primarily as membrane anchors [31, 32]. In addition, our results indicate that the MgrB TM region together with the small cytoplasmic region interacts with PhoQ, and that residue W20 in the TM region is essential for MgrB/PhoQ complex formation. Tryptophan is often found in transmembrane proteins, especially at the ends of TM helixes as a membrane anchor due to its unique amphipathic side chain [45, 46]. W20 in MgrB does not appear to position near the computationally predicted membrane/periplasm interface. It is possible that the unique side chain of W20 interacts with polar and/or aromatic residues in the PhoQ transmembrane domain, such as the functionally important N202 [47]. The mechanism of how W20 mediates PhoQ/MgrB complex formation awaits further investigations.

437 We identified two lysines in the MgrB cytosolic region that are important for the protein's
438 function. Although these residues are not individually essential, replacing both with
439 negatively charged residues significantly affected MgrB activity. A screen for PhoQ mutants
440 that increase the inhibitory activity of MgrB K2DK3D identified R219 in PhoQ. When this
441 residue was mutated to a negatively charged amino acid, the inhibitory activity of MgrB
442 K2DK3D was partially restored, suggesting the possibility that MgrB inhibitory activity of
443 PhoQ is in part mediated by charge-charge repulsion between K2K3 in MgrB and R219 in
444 the PhoQ TM2-HAMP junction. This hypothesis is consistent with the observation that K2
445 and K3 did not contribute to MgrB/PhoQ complex formation, since the HAMP domain is
446 conformationally dynamic and transduces signals via conformational changes [44, 48]. It is
447 also noteworthy that the TM2-HAMP junction has been reported to be essential for signaling
448 by other membrane proteins such as the chemoreceptor Tar [49]. In fact, some modifications
449 of the TM2-HAMP junction result in signal inversion in *E. coli* [49]. The partial suppression by
450 PhoQ R219D indicates the existence of other factors involved in PhoQ/MgrB interaction at
451 this residue. Mutating arginine to aspartate not only changes the charge but also the length
452 of the side chain (as well as other properties), which may have an impact on PhoQ/MgrB
453 interaction. Interestingly, we observed activity inversion (from activation to inhibition) of MgrB
454 K2DK3D when increasing its expression. Considering its reduced membrane localization
455 and possible heterogeneous cell population under arabinose induction, it is possible that the
456 mild activating activity we observed for lower expression level was due to factors other than
457 the direct effects of the mutant MgrB on PhoQ. Alternatively, different amounts of MgrB
458 K2DK3D might lead to different energy states or conformations of the PhoQ TM2-HAMP
459 junction, and thus changes in PhoQ activity. Lastly, we note that some MgrB orthologs have
460 a longer N-terminal cytosolic region and some do not have positive charged residues at
461 position 2 and 3. Due to the dynamic nature of the HAMP domain and the TM2-HAMP
462 junction, it is possible that these MgrB orthologs have different interactions with PhoQ.
463
464 Previous work indicates that the periplasmic region of MgrB and, in particular, two conserved
465 cysteines in this region, are critical for PhoQ inhibition [18, 20]. To identify other periplasmic
466 residues in MgrB that are required for PhoQ inhibition, we analyzed individual alanine
467 substitutions across the entire periplasmic region. Remarkably, despite the small size of this
468 region and the level of conservation, substitutions at most positions had little effect on MgrB
469 activity. Of the 22 residues in the periplasmic region, only six were individually important for
470 full activity: the two conserved cysteines (C28 and C39), as previously noted [20], as well as
471 G37, D31, F34 and W47. Furthermore, substitutions at these latter four residues lowered but
472 did not eliminate MgrB activity. Interestingly, mutations for each of these positions are also
473 associated with colistin-resistant *Klebsiella* isolates [23, 24, 50-55]. Taken together, our
474 findings show that the sequence determinants for MgrB activity are not restricted to either
475 one of the regions – cytosolic, periplasmic or TM, and that functionality is mediated by
476 collective interactions of key amino acid residues scattered across the polypeptide.
477
478 We also tested a number of MgrB orthologs derived from other enterobacteria with varying
479 sequence similarity to *E. coli* MgrB. Most orthologs that we tested efficiently inhibited *E. coli*
480 PhoQ. The slight decrease in activities of *K. pneumoniae* and *S. typhimurium* MgrB could be
481 due to the presence of a glycine residue within the TM regions, which may affect the
482 conformational flexibility of the TM helix and cause a defect in binding and inhibiting PhoQ.
483 On the other hand, *Y. pestis*, *P. penneri* and *P.stuartii* MgrB appear to be more efficient than
484 *E. coli* MgrB in inhibiting *E. coli* PhoQ. It is notable that the tryptophan residue (W20) found
485 in the TM region of *E. coli* MgrB is replaced by a tyrosine (Y20) in these orthologs. It is
486 possible that a hydrogen bond involving Y20 or the smaller size of tyrosine relative to
487 tryptophan affects the interaction of MgrB with PhoQ.
488
489 Unexpectedly, we also found that MgrB lacking its periplasmic region, as well as full-length
490 MgrB, interact with several other histidine kinases in addition to PhoQ in a bacterial two-
491 hybrid assay. However, we did not observe a significant effect of MgrB on gene expression

492 regulated by these histidine kinases. The TM domains of many dimeric histidine kinases
493 such as PhoQ and EnvZ are believed to form a four-helix bundle [48]. Our results may
494 reflect an interaction between the MgrB TM and a conserved conformation of the
495 transmembrane domain shared by multiple histidine kinases. The cytosolic and periplasmic
496 regions of MgrB apparently provide additional interactions required for specific regulation of
497 PhoQ. It will be interesting to determine if there are other small membrane proteins that have
498 evolved to interact with other histidine kinases using structural features similar to those of
499 the MgrB TM region. In addition, the results from our study of MgrB, as well as studies of
500 other small membrane proteins, may provide a platform for reengineering these proteins to
501 regulate new targets through rational design and directed evolution.
502

503 ## Materials and Methods

504

505 **Strains, plasmids and cloning**

506 See Supporting information for tables of strains (S1 Table), plasmids (S2 Table), and
507 primers (S3 Table) used in this study. All strains were derived from *E. coli* K-12 MG1655.
508 Gene deletions and reporter constructs were transferred between strains using transduction
509 with $P1_{vir}$. Deletions in the Keio collection [56] that were used for strain construction were
510 confirmed by PCR using primers flanking the targeted gene. Kanamycin resistance markers
511 were excised, when required, using the FLP-recombinase-expressing plasmid pCP20
512 [57]. Strain SAM72 was constructed by first excising the kanamycin resistance cassette from
513 the *ompC-mCherry* transcriptional reporter strain AFS256 to give SAM71. Kanamycin
514 resistance from the *mzrA* deletion strain JW3067 was then transduced into SAM71 by P1
515 transduction. A deletion of *safA* (SAM73) was constructed as described in [28, 57]. SAM73
516 was then used to construct SAM76 by transducing the *mgtA-lacZ* transcriptional reporter
517 from TIM199. Strain SAM85, which is a *lacI*^{q} containing version of BTH101 was made by
518 conjugation of the bacterial two-hybrid host strain BTH101 (F−) with XL1-Blue (F+). This
519 strain was used instead of BTH101 as it gave reduced background in our MacConkey plate
520 assays. Strain JingY90 was constructed by introducing *phoQ* deletion to JingY34 using P1
521 transduction followed by kanamycin resistance cassette removal. Plasmids expressing
522 *gfpA206K* fusions to *mgrB* mutants (pSY3-9, pSY72-75, pJC1-7, pTG1-15) were created by
523 either QuikChange site-directed mutagenesis (Stratagene) or Inverse PCR [58] using pAL38
524 as template. Plasmids expressing *gfpA206K* fusions of *mzrA* (pSY29)), *safA* (pSY31) and
525 *mgrB* orthologs (pSV1-8) were constructed by Gibson assembly [59].The gene fragments for
526 *mzrA* and *safA* were PCR amplified from the MG1655 genome, and gene fragments
527 corresponding to the different *mgrB* orthologs were synthesized commercially (Integrated
528 DNA Technologies, Inc.).Plasmids pSY32 (MzrA TM swap) and pSY33 (SafA TM swap)
529 were made by Inverse PCR using pSY29 and pSY31 as templates, respectively. Plasmid
530 pSY34 expressing T18-MgrB-24 only was created using pAL33 as template by Inverse PCR.
531 For all the plasmids mentioned above, see S3 Table for specific primer sequences used for
532 each construction. Plasmids pSY61, pSY64 and pSY68 were constructed as follows: *atoS*,
533 *cpxA*, and *phoR* were PCR-amplified using MG1655 genome as the template and the
534 following primer pairs – atoS-xbaI-U1/atoS-kpnI-L1, cpxA-xbaI-U1/cpxA-kpnI-L1 and phoR-
535 xbaI-U2/phoR-kpnI-L1, respectively, digested with XbaI/KpnI restriction enzymes and then
536 cloned into pKT25 at XbaI/KpnI sites. Plasmid pJY151 was constructed by inserting PCR
537 amplified *mgrB* to SacI/XbaI sites in pBAD33RBS vector. Plasmid pJY569 expressing
538 *mcherry-mgrB* was generated by inserting *mgrB* downstream of *mcherry* at BamHI/PstI sites
539 in pBO2 [60]. Plasmid pJY573 was generated by inserting *mNeonGreen* downstream of
540 phoQ at SalI/HindIII sites in pBAD33RBS phoQ [14]. Plasmids expressing *mgrB* variants
541 were constructed using Q5 site-directed mutagenesis kit (NEB). All constructs were
542 confirmed by DNA sequencing.
543

544 **Media and growth conditions**

545 Liquid cultures were grown at 37 °C with aeration, unless otherwise indicated, in either LB
546 Miller medium (Fisher Scientific) or in minimal A medium [61] containing 0.2% glucose, 0.1%
547 casamino acids and 1 mM $MgSO_4$. For routine growth on solid medium, LB or minimal
548 medium containing bacteriological grade agar (Fisher Scientific) was used. The antibiotics
549 ampicillin, kanamycin and chloramphenicol were used at concentrations 50–100, 25-50 and
550 20–34 μg mL^{-1}, respectively. The *lac* and *trc* promoters were induced with isopropyl *β*-D-1-
551 thiogalactopyranoside (IPTG) at a final concentration of 10 μM in FRET analysis or 1 mM
552 when indicated. When IPTG was not mentioned in the description of the culture conditions,
553 the basal transcription from the *trc* promoter was used to drive expression. The araBAD
554 promoter was induced with 0.008% arabinose. For bacterial two-hybrid screening,
555 MacConkey/maltose indicator plates were prepared as described [36] using MacConkey
556 agar base powder (Difco™), 100 μg mL^{-1} ampicillin, 25 μg mL^{-1} kanamycin, 0.5 mM IPTG
557 and 1% maltose.
558
559 **β-galactosidase reporter gene assay**
560 Cultures of strain AML67 carrying *gfpA206K* fusions of either wild-type *mgrB* (pAL38), *mgrB*
561 mutants (pSY3-9, pSY72-75, pJC1-7, pTG1-15), *mgrB* orthologs (pSV1-8) or *gfpA206K*-only
562 (pAL39) plasmids were grown overnight in LB with 50 μg mL^{-1} ampicillin. The next day, they
563 were diluted 1:1000 into the same medium and grown to OD_{600} ~0.3-0.4 at 37 °C. Cells were
564 permeabilized with chloroform/SDS and assayed as in [61]. For high-throughput
565 measurements in a 96-well format, the protocol was modified as described in Thibodeau *et*
566 *al*.[62].
567
568 **GFP reporter assay**
569 *E. coli imp-4213* strain carrying GFP reporter plasmid (pUA66 P_{mgtLA}-*gfp*) was grown
570 overnight at 37 °C in Luria–Bertani (LB) medium supplemented with 1 or 10 mM $MgSO_4$,
571 then diluted 1:100 to fresh $MgSO_4$ supplemented LB medium. DMSO, MgrB or SafA C-
572 terminal peptides (synthesized by Genscript) were added to the culture with indicated
573 amount. The cultures were grown at 37 °C with vigorous shaking for two hours. The
574 fluorescence of cells was then monitored with a BD LSRFortessa SORP flow cytometer (BD
575 Biosciences) and the acquired data were analyzed as described before [14]. To test the
576 function of MgrB variants, *E. coli* MG1655 *ΔmgrB* strain was transformed with GFP reporter
577 plasmid (pUA66 P_{mgtLA}-*gfp*) [14] and a pBAD33 vector carrying wild-type or mutant *mgrB*
578 genes. The resulting transformants were grown overnight at 37 °C in LB medium
579 supplemented with 10 mM $MgSO_4$, then diluted 1:100 to fresh LB medium supplemented
580 with 1 mM $MgSO_4$ and 0.008% arabinose. The cultures were grown at 37 °C with vigorous
581 shaking for two hours to reach early log phase (OD=0.4-0.5). The fluorescence of cells was
582 monitored and the acquired data were analyzed as described before [14]. The normalized
583 MgrB mutant activity was calculated as following:
584 $Activity^{mut} = (Fluorescence^{no_MgrB_control} - Fluorescence^{MgrB_mut}) / (Fluorescence^{no_MgrB_control} -$
585 $Fluorescence^{MgrB_WT}) \times 100\%$
586 Where appropriate, 50 μg mL^{-1} kanamycin and 34 μg mL^{-1} chloramphenicol was added to
587 the growth media.
588
589 **Acceptor photobleaching FRET analysis**
590 The expression of PhoQ-mNeonGreen and mCherry-MgrB was induced in *E. coli*
591 ΔphoQΔmgrB strain with 0.008% arabinose and 10 μM IPTG, respectively. The cultures
592 were grown to mid-log phase (OD=0.6) in LB media supplemented with 10 mM $MgSO_4$ and
593 appropriate antibiotics. Cells were harvested and washed two times with pre-chilled tethering
594 buffer (20 mM potassium phosphate pH7.0, 1 μM methionine, 10 mM lactic acid and 10 mM
595 magnesium sulfate). The surface of a glass-bottom 24-well plate (Greiner) was treated with
596 0.1% poly-L-lysine (Sigma) for 10 minutes at room temperature followed by rinsing with
597 tethering buffer. Cells were then added to the wells and incubated at room temperature for
598 10 minutes to allow attachment. Unattached cells were removed by washing two times and
599 attached cells were overlaid with tethering buffer afterwards.

Acceptor photobleaching FRET was performed using a dual layer Nikon Ti-E inverted fluorescence microscope equipped with a fluorescence lamp (X-cite Exacte, Lumen Dynamics), Perfect Focus System (PFS) and NIS-Elements AR software (version 4.40 Nikon). Images were acquired through a 40x Plan Apo NA 0.95 objective in the mNeonGreen (donor) and mCherry (acceptor) channels, excitation power was adjusted both by controlling the fluorescence lamp output and with ND filters. Specifically, the donor was excited at 482/18 nm and its emission was detected at 525/50 nm and the acceptor was excited at 585/29 while its emission was detected at 647/57. Excitation and emission filters were mounted respectively on excitation and emission filter wheels, while beam splitters (495LP for mNeonGreen excitation and 605LP for mCherry excitation) were on the lower dichroic wheel of the microscope. Images were recorded using an iXon 897-X3 EM-CCD camera (Andor), the acquisition time was set to 1 second for both channels and EM gain was kept in the range of 100-280. Acceptor (mCherry) photobleaching was induced by a 150 mW DPSS 593 nm laser (ACAL Bfi) that was reflected on the sample by a zt594 DCRB laser beam splitter (AHF) mounted on the upper dichroic wheel.

For each well we acquired two to three sequences of images on isolated sample areas with the following protocol: (a) first, two images were taken in the acceptor channel; (b) then sixty images were taken in the donor channel followed by (c) ten seconds acceptor photobleaching (no image acquisition); afterwards, (d) forty images were taken in the donor channel; and then (d) two images were taken in the acceptor channel. In order to avoid donor fluorescence recovery from interrupted illumination, the sample was continuously illuminated with a 482/18 nm excitation light, even during step (c). FRET efficiency was calculated as the donor signal increase divided by the total donor signal after acceptor photobleaching. In order to correct for the donor photobleaching present during steps (b) to (d), we performed linear fitting (RStudio) of the donor fluorescence signal versus time for both pre- and post-bleaching curves.

Bacterial two-hybrid assays

For the colorimetric spot assay, multiple clones from the transformation plate were inoculated in 3 mL of LB containing 100 µg mL^{-1} ampicillin and 25 µg mL^{-1} kanamycin. (Several clones were picked in order to reduce heterogeneity [36]. Cultures were grown overnight at 30 °C with shaking. The next day, 3 µL of each culture was spotted on MacConkey/maltose indicator plates and plates were then incubated at 30 °C. For each pair of plasmids, triplicate experiments were performed. Color change on the indicator plates was recorded after 48 h of incubation. Alternatively, *β*-gal assays were performed on the overnight liquid cultures prepared as described for the colorimetric assay.

Random mutagenesis of the PhoQ TM2-HAMP region

The GeneMorph II random mutagenesis kit (Stratagene) was used to mutagenize the TM2-HAMP-encoding region of *phoQ* (in pBAD33 *phoQ*) using primers that specifically target this region. The library was transformed into an *E. coli ΔphoQΔmgrB* strain carrying a plasmid GFP reporter (pUA66 *PmgtL-gfp*) and an MgrB K2DK3D expression plasmid (pTrc99a *mgrB K2DK3D*). The transformants were grown on LB plates containing arabinose to induce PhoQ expression. *E. coli* colonies with repressed PhoQ have weak green fluorescence. Dim colonies were selected and their plasmids were sequenced to identify mutations in PhoQ. Site-directed mutagenesis was performed using Q5 site-directed mutagenesis kit (NEB).

Acknowledgements

We thank J. Zhu for the BACTH plasmid pKT25-toxR; S. Hoch and S. G. Sierra for technical assistance; members of the Goulian, Sourjik, Zhu and Binns labs for helpful discussions; P. Shah for a critical reading of the manuscript. This work was supported by NIH award

GM118059 (to B.N.), NIH award GM080279 (to M.G.) and NSF award DMR11-20901 (to M.G.).

Author contributions

S.S.Y., J.N.C. V.S., J.Y. and M.G. designed the experiments. S.S.Y., J.Y., G.M., T.G., S.V. and J.N.C. performed the experiments. B.N. contributed new reagents/analytical tools. S.S.Y., T.G., S.V., J.N.C., G.M., V.S., J.Y. and M.G. analyzed the data. S.S.Y., J.Y., V.S., M.G. wrote the manuscript and all authors edited the manuscript.

Figures

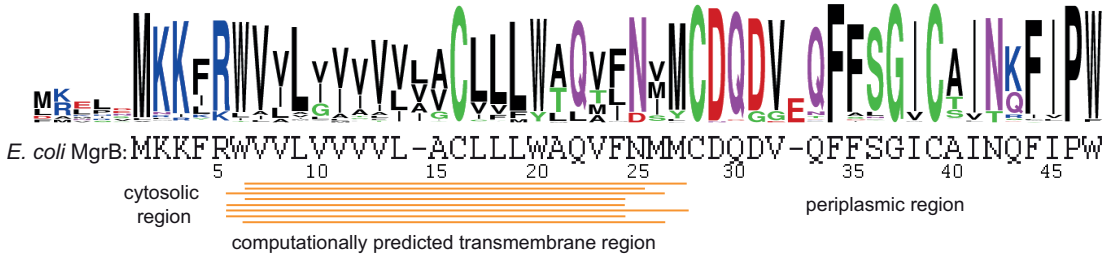

Fig 1. The conservation of MgrB sequence
The sequence logo of MgrB generated with bacterial MgrB sequences obtained from KEGG protein BLAST using *E. coli* MgrB as query highlights the degree of amino acid conservation. The MgrB sequences and multiple sequence alignment can be found in the supplementary file (MgrB_alignment).

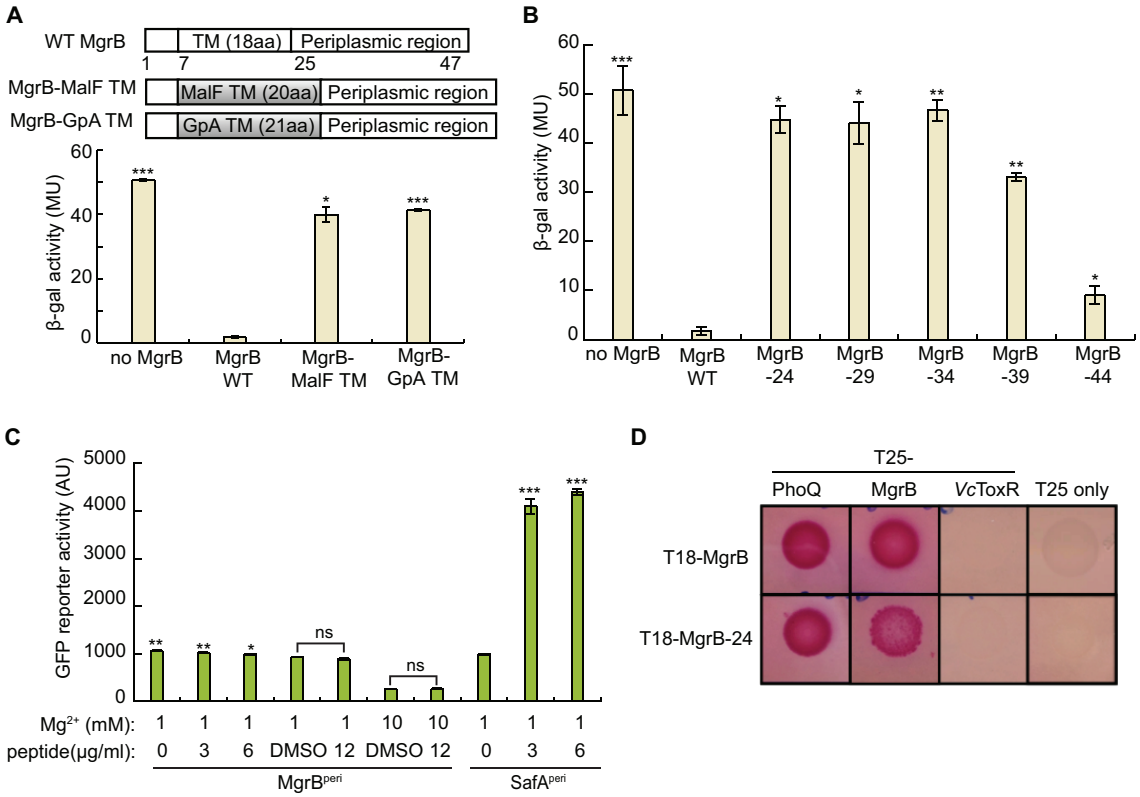

Fig 2. The MgrB transmembrane domain and periplasmic domain are essential but not sufficient for its function as a PhoQ inhibitor.

A, Schematic representation of transmembrane (TM) domain swap constructs to replace the MgrB TM sequence with TM sequences derived from either the protein MalF or human glycophorin A, GpA. β-galactosidase activities of wild-type MgrB (pAL38), its variants MgrB-MalF TM (pSY3), MgrB-GpA TM (pSY4) and no MgrB control (pAL39) in a Δ*mgrB* strain containing a PhoQ/PhoP-regulated transcriptional reporter P_{mgtA}-*lacZ* (AML67) is shown below. Inducer was not added as the leaky expression from the *trc* promoter resulted in sufficient levels for strong inhibition by WT MgrB. Data represent averages and ranges for two independent experiments. MU = Miller Units. **B**, effect of wild-type MgrB and the truncation mutants were measured in a Δ*mgrB* strain containing the PhoQ/PhoP-regulated transcriptional reporter P_{mgtA}-*lacZ* (AML67) as in **A**. **C**, the activities of $MgrB^{Peri}$ and $SafA^{Peri}$ were monitored using PhoQ/PhoP-regulated transcriptional reporter P_{mgtLA}-*gfp*. Peptides or DMSO were added to the *E. coli imp4213* culture with indicated amount. The GFP activities were measured after 2h incubation using flow cytometry. Data points represent averages of three independent experiments and error bars show SDs. **D**, bacterial two-hybrid (BACTH) colorimetric spot assays with cells expressing protein fusions to the T18 and T25 subunits of *B. pertussis* adenylyl cyclase. Representative images showing interactions between MgrB-24 (T18-MgrB-24) and partner proteins PhoQ (T25-PhoQ) and MgrB (T25-MgrB). Interactions between MgrB-PhoQ, MgrB-MgrB, MgrB-T25 only and (MgrB-24)-T25 only were included as positive and negative controls. As an additional control, interactions were tested between MgrB-24 and *Vibrio cholerae* membrane protein ToxR (*Vc*ToxR), and also between MgrB and *Vc*ToxR . Each pair of interactions was assayed in at least three independent trials in a *cyaA*$^-$ BACTH host strain containing *lacI*^{q} (SAM85), on maltose MacConkey indicator plates (results from one representative experiment are shown). The plates were incubated at 30°C for 48 h before images of plates were acquired. The pink color indicates reconstitution of adenylyl cyclase activity. The statistical significances of changes in reporter

activity were calculated with *t* tests by comparing to wild type (in A, B) or to the DMSO negative control (in C) and indicated with asterisks (*** $P \leq 0.001$, ** $P \leq 0.01$, * $P \leq 0.05$, ns = not significant) in A, B and C.

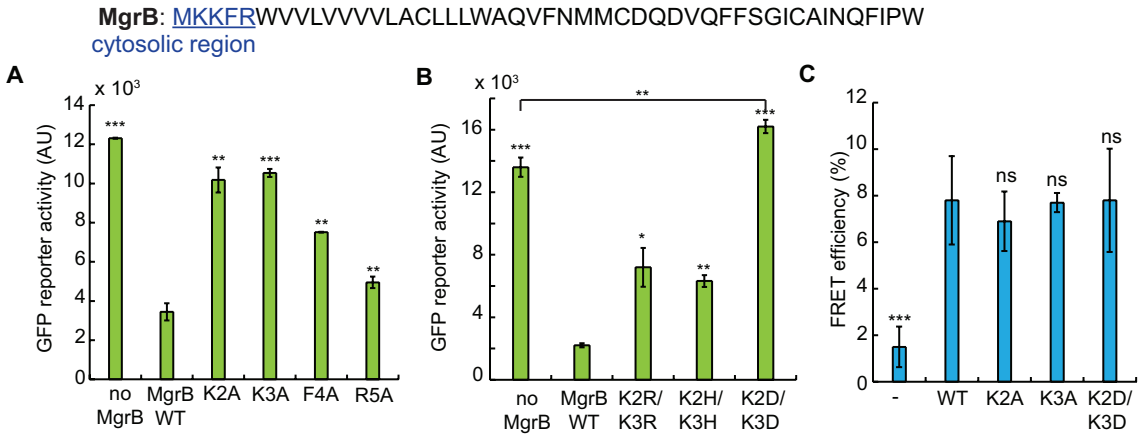

Fig 3. Two lysines in MgrB cytosolic region regulate PhoQ activity through their charged side chain.

A, the activities of MgrB mutants with single alanine substitution in the cytosolic region were tested using the PhoQ/PhoP-regulated transcriptional reporter P_{mgtLA}-*gfp* in a Δ*mgrB* strain. MgrB mutants were constructed in a pBAD33 vector and their expression was induced with 0.008% arabinose. **B**, the activities of MgrB K2K3 double mutants were tested as in **A.** The reporter activity change was significant (P = 0.0045) when comparing MgrB K2DK3D to the no_MgrB control. **C**, FRET efficiencies were measured between PhoQ-mNeonGreen and mCherry (-), wild-type MgrB (WT) or MgrB mutants (K2A, K3A, K2DK3D and K2EK3E). MG1655 Δ*phoQ* Δ*mgrB* strain was transformed with pBAD33 *phoQ-mneongreen* and pTrc99a *mcherry-mgrB* variants. Protein expression was induced with 0.008% arabinose and 10 μM IPTG. FRET was measured for each protein pair and the efficiencies were calculated as described in Materials and Methods. All data points represent averages of at least three independent experiments and error bars show SDs. The statistical significances of changes in reporter activity or FRET efficiency were calculated with *t* tests by comparing to wild type or as specified and indicated with asterisks (*** $P \leq 0.001$, ** $P \leq 0.01$, * $P \leq 0.05$, ns = not significant).

MgrB: MKKFRWVVLVVVVLACLLLWAQVFNMMCDQDVQFFSGICAINQFIPW
predicted TM region

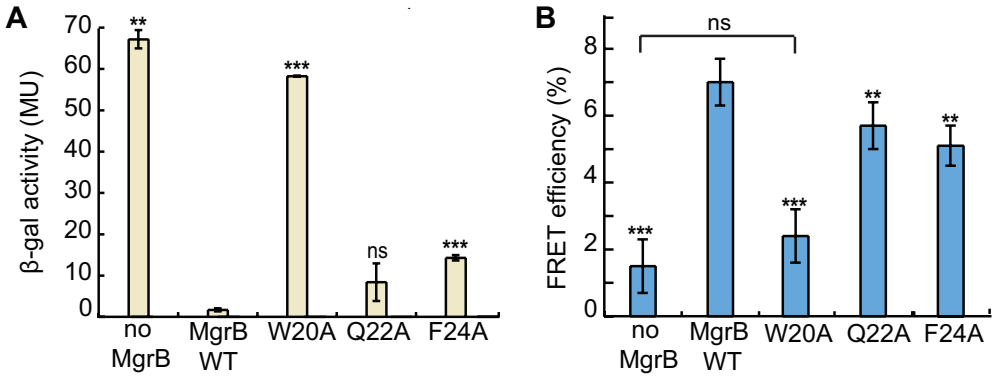

Fig 4. W20 in MgrB transmembrane domain is essential for PhoQ/MgrB complex formation.

A, β-galactosidase levels were measured in a Δ*mgrB* strain containing the PhoQ/PhoP-regulated transcriptional reporter P_{mgtA}-*lacZ* (AML67) and also containing either an empty vector (pAL39), wild-type MgrB (pAL38), or the indicated mutants MgrB W20A (pSY72), Q22A (pSY73) and F24A (pSY74). Inducer (IPTG) was not added as the leaky expression from the *trc* promoter resulted in sufficient levels of protein. Mutants with β-galactosidase activity ≥ 5-fold above wild type were selected for further analysis. Data represent averages and ranges for two independent experiments. MU = Miller Units. **B**, FRET efficiencies were measured between PhoQ-mNeonGreen and indicated mCherry-MgrB variants as described in Figure 3C. When compared to wild type, the reduction of FRET efficiencies is significant according to *t* test (*** $P < 0.001$, ** $P < 0.01$). Data points represent averages of at least three independent experiments and error bars show SDs. The statistical significances of changes in reporter activity or FRET efficiency were calculated with *t* tests by comparing to wild type and indicated with asterisks (*** $P \leq 0.001$, ** $P \leq 0.01$, * $P \leq 0.05$, ns = not significant).

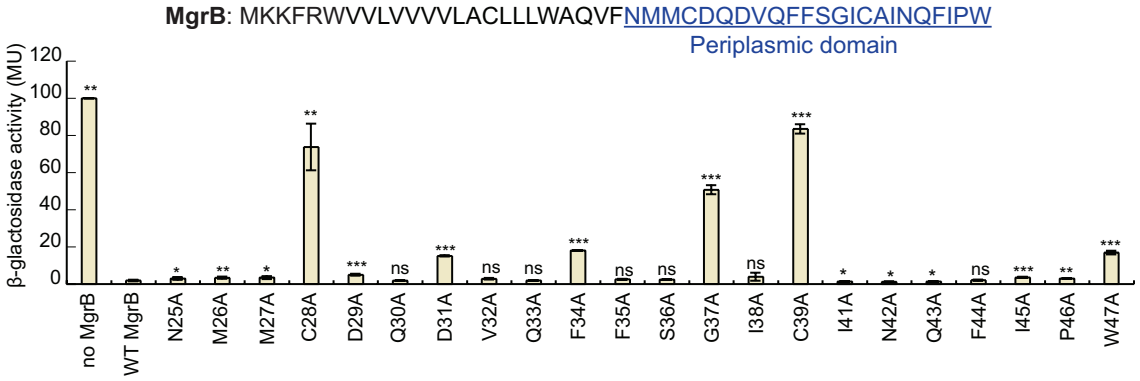

Fig 5. Effects of site-directed alanine substitutions of MgrB periplasmic residues on PhoQ activity.

β-galactosidase levels were measured in a Δ*mgrB* strain containing the PhoQ/PhoP-regulated transcriptional reporter P_{mgtA}-*lacZ* (AML67) and also containing either an empty vector (pAL39), wild-type MgrB (pAL38), or the indicated mutants (pJC1 through pJC7 and pTG1 through pTG15; see Table S2 for details). Inducer (IPTG) was not added as the leaky expression from the *trc* promoter resulted in sufficient levels of protein. Data for wild-type MgrB and each mutant was normalized to the no-MgrB control. Mutants with β-galactosidase activity ≥ 5-fold above wild type were selected for further analysis. Averages and standard deviations for three independent experiments are shown. MU = Miller Units. The statistical significances of changes in reporter activity were calculated with *t* tests by comparing to wild type and indicated with asterisks (*** $P \leq 0.001$, ** $P \leq 0.01$, * $P \leq 0.05$, ns = not significant).

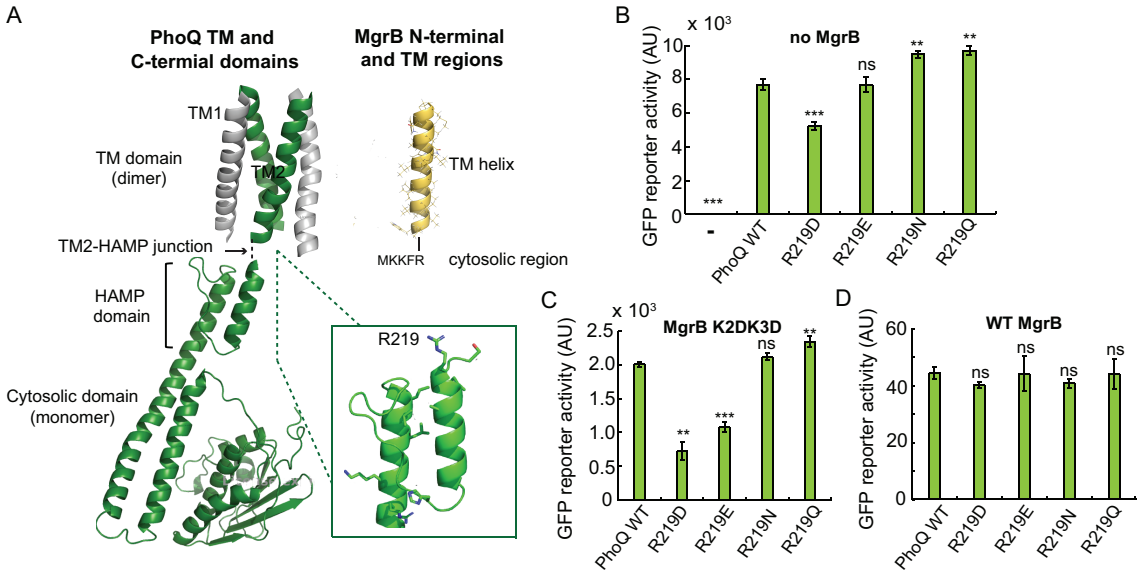

Figure 6. PhoQ R219 is involved in interactions with MgrB K2 and K3.
Models of TM [14] and cytosolic domains [44] of PhoQ and MgrB are shown in (**A**)**.** The MgrB TM model was constructed *ab initio* via Rosetta (https://www.rosettacommons.org). PhoQ R219 residue is labeled and shown with side chain in a zoomed-in view. **B**, the activity of PhoQ R219 mutants was tested using the PhoQ/PhoP-regulated transcriptional reporter P_{mgtLA}-*gfp* in a Δ*phoQ*Δ*mgrB* strain. PhoQ mutants were expressed from the plasmid pBAD33 with 0.008% arabinose. The activities of PhoQ R219 mutants were tested in the presence of MgrB K2DK3D (**C**) or wild type (**D**) using the same GFP reporter as in **B**. MgrB variants were expressed from a pTrc99a vector with no inducer (IPTG) added, as the leaky expression from the *trc* promoter resulted in sufficient levels of protein. Averages and standard deviations for three independent experiments are shown in **B**-**D**. The statistical significances of changes in reporter activity were calculated with *t* tests by comparing to wild type and indicated with asterisks (*** $P \leq 0.001$, ** $P \leq 0.01$, * $P \leq 0.05$, ns = not significant).

A

```
Escherichia coli         ---MKKFRWVVLVVVVLACLL-LWAQVFNMMCDQDV-QFFSGICAINQFIPW---
Klebsiella pneumoniae    ---MKKLRWVLLIVIIAGCLL-LWTQMLNVMCDQDV-QFFSGICTINKFIPW---
Yersinia pestis          MLDLNITKLVTTVVIIAACCL-FYLLALDSYCDQGG-TFSTGICAITTIVPW---
Photorhabdus laumondii   ---MDIKKTIAILALLGICLF-LYLLALDSYCDQGE-QFDSGICSVTRYLPF---
Proteus penneri          ---MNAKKIIISLIIALVITFGLYLVALDNFCDRGE-DFQQGLCRFTTLFPSKHH
Providencia stuartii     ---M-KYKLIIGVCIVITCIF-LYLLAMDSLCDQGGENFIFGICQITDLLPF---
Serratia sp. MYb239      ---MLRNKILLIVATVLACLF-FNLLALDSYCDQGG-NFALGICSITRIIPW---
Enterobacter ludwigii    -----------MIIVLVACVV-LWTQTINVMCDQDV-QFFSGVCAINKFIPW---
Salmonella typhimurium   ---MKKFRWVVLGIVVVVCLL-LWAQVFNIMCDQDV-QFFSGICAINKFIPW---
                                                . :    ::  **..   *  *:* ..  .*
```

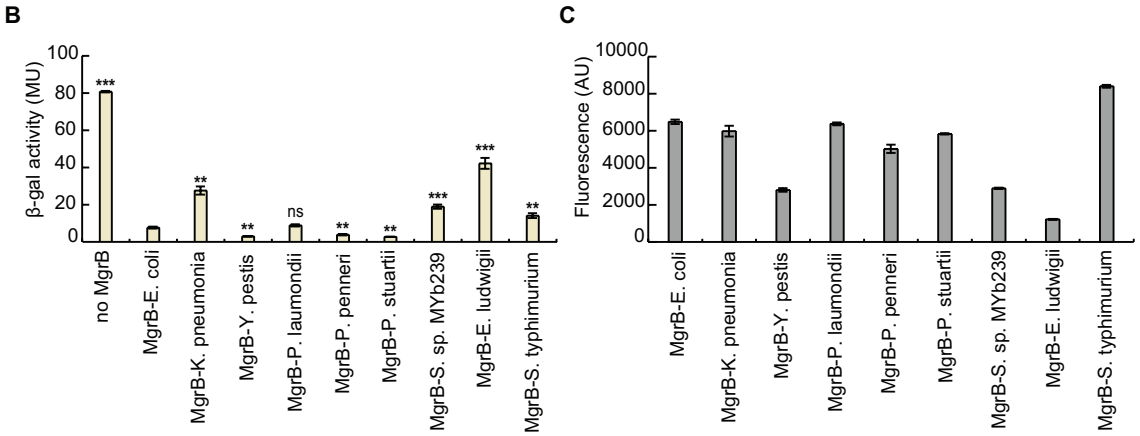

Figure 7. Effect of MgrB orthologs on *E. coli* PhoQ activity.
A, Sequence alignment of MgrB orthologs. **B**, β-galactosidase levels of a Δ*mgrB* strain containing the PhoQ/PhoP-regulated transcriptional reporter P_{mgtA}-*lacZ* (AML67) and also containing either an empty vector (pAL39), wild-type MgrB (pAL38), or a plasmid expressing the indicated MgrB orthologs. Inducer (IPTG) was not added as the leaky expression from the *trc* promoter resulted in sufficient levels of protein. Averages and standard deviations for three independent experiments are shown. MU = Miller Units. The statistical significances of changes in reporter activity were calculated with *t* tests by comparing to wild type and indicated with asterisks (*** $P \leq 0.001$, ** $P \leq 0.01$, * $P \leq 0.05$, ns = not significant). **C**, GFP-MgrB expression levels for cells expressing MgrB orthologs were imaged by fluorescence microscopy, and GFP fluorescence levels were quantified (see Methods for details). Data represent averages and ranges for two independent experiments comprised of 200 cells each, AU = Arbitrary Units.

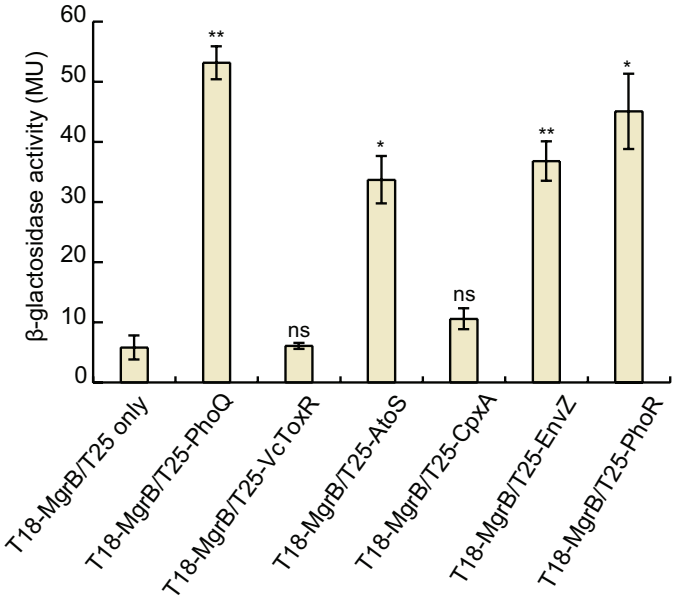

Figure 8. MgrB interacts with other histidine kinases in a bacterial two-hybrid assay. Bacterial two-hybrid (BACTH) assays with cells expressing protein fusions to the T18 and T25 subunits of *B. pertussis* adenylyl cyclase. β-gal expression from the *lac* promoter was monitored as a measure of interactions between T18-MgrB and T25 fusion with either PhoQ, AtoS, CpxA, EnvZ or PhoR. The T25 fragment alone and T25-*Vc*ToxR (*Vibrio cholerae* ToxR) serve as negative controls. β-gal assays were carried out in a *cyaA*$^-$ BACTH host strain containing *lacI*^{q} (SAM85). Data represent averages and ranges for two independent experiments. MU = Miller Units. The statistical significances of changes in reporter activity were calculated with *t* tests by comparing to the negative control (T18-MgrB/T25 only) and indicated with asterisks (*** $P \leq 0.001$, ** $P \leq 0.01$, * $P \leq 0.05$, ns = not significant).

Supporting information

S1 Text. Materials and methods

Fluorescence microscopy

Strains were grown in minimal medium containing with antibiotics as needed and single-cell measurements were performed essentially as described previously [21]. For MgrB localization experiments, saturated overnight cultures of AML67 strains carrying *gfpA206K* fusions of either wild-type *mgrB* (pAL38), *mgrB* mutants (pSY3-9, pSY72-75, pJC1-7, pTG1-15) , *mgrB* orthologs (pSV1-8) or *gfpA206K*-only (pAL39) were diluted 1:1,000 into fresh medium containing 100 μg mL^{-1} ampicillin and grown at 37 °C with aeration to an OD_{600} ~0.2–0.3 (~4-5 h) before visualization. For single-cell fluorescence measurements from transcriptional reporter strains, cultures were grown as outlined above, then rapidly cooled in an ice-water slurry and streptomycin was added to a final concentration of 250 μg mL^{-1} to stop protein synthesis. Microscope slides were prepared with 1% agarose pads and cell fluorescence was measured by imaging and quantified with in-house software as described previously [21, 63].

Membrane protein isolation and Western blot analysis

Cells expressing Flag tagged MgrB variants were harvested and resuspended in lysis buffer (50mM Tris-Cl pH8.0, 100 mM NaCl and protease inhibitors). The membrane fraction was collected as described before with modifications [34]. Specifically, cells were disrupted by homogenization at 4 °C and cell debris were remove by centrifugation at 2,300 x g for 10 minutes. The lysate was centrifuged again at 21,000 x g for 60 minutes at 4 °C to pellet the membrane fraction. The membrane pellet was washed with 1 ml lysis buffer and dissolved in SDS sample buffer overnight at 4 °C. The samples were heated at 60 °C for 10 minutes and the proteins were separated on a 16% tricine gel. The separated proteins were then transferred to Immobilon-P^{SQ} PVDF membrane (Merckmillipore) in transfer buffer containing 20% methanol and Flag-flexilinker-MgrB was detected with anti-Flag primary antibody (Sigma) and IRDye 800CW-conjugated secondary antibody (LI-COR). The protein bands were visualized with the Odyssey CLx imaging system (LI-COR) and quantified with ImageJ.

S1 Table. Strains

Strain	Genotype	Source or Reference
AFS256	MG1655 λ_{att}::(P_{ompC}-*mCherry FRT-kan-FRT*)	Goulian lab collection
AML67	MG1655 Δ*mgrB*::(*FRT-kan-FRT*) Δ*lacZ* λ_{att}::(P_{mgtA}-*lacZ cat*)	[18]
BTH101	F-, *cya-99 araD139 galE15 galK16 rpsL1* (Str^r) *hsdR2 mcrA1 mcrB1*	Euromedex
BW25113	*rrnB3* Δ*lacZ4787 hsdR514* Δ(*araBAD*)*567* Δ(*rhaBAD*)*568 rph-1*	[64]
JW3067	BW25113 Δ*mzrA*::(*FRT-kan-FRT*)	KEIO collection [56]
MG1655	F^- λ^- ilvG- rfb-50 rph-1	*E. coli* Genetic Stock Center, CGSC# 7740
SAM71	MG1655 λ_{att}::(P_{ompC}-*mCherry*)	This study
SAM72	MG1655 Δ*mzrA*::(*FRT-kan-FRT*) λ_{att}::(P_{ompC}-*mCherry*)	This study
SAM73	MG1655 Δ*safA*::(*FRT-kan-FRT*)	This study
SAM76	MG1655 Δ*safA*::(*FRT-kan-FRT*) Δ*lacZ* λ_{att}::(P_{mgtA}-*lacZ cat*)	This study
SAM85	F+ *lacI*^{q}ZΔ*M15* Tn*10* (Tet^r), *cya-99 araD139 galE15 galK16 rpsL1* (Str^r) *hsdR2 mcrA1 mcrB1*. Strain prepared by conjugation: BTH101 (F-) x XL1-Blue (F+).	This study

TIM199	MG1655 Δ*lacZ* λ_{att}::(P_{mgtA}-*lacZ cat*)	[18]
XL1-Blue	*recA1 endA1 gyrA96 thi-1 hsdR17 supE44 relA1 lac* [F´ *proAB lacI*^{q}*Z*Δ*M15* Tn*10* (Tet^r)]	[65]
Imp-4213	F-, *lptD4213*, *galK2*(Oc), *λ*$^-$, *IN(rrnD-rrnE)1*, *rpsL200*(strR), *rph-1*	[35]
JingY34	MG1655 Δ*mgrB::FRT*	[14]
JingY90	MG1655 Δ*phoQ::FRT* Δ*mgrB::FRT*	This study

S2 Table. Plasmids

Plasmid	Relevant genotype	Source or Reference
pAL25	pKT25 P_{lac}-*cyaA*$_{T25}$-*mgrB*, Kan^R	[18]
pAL27	pKT25 P_{lac}-*cyaA*$_{T25}$-*phoQ*, Kan^R	[18]
pAL30	pBAD33 P_{araBAD}-*phoQ(his)*$_6$, Cam^R	Goulian lab collection
pAL33	pUT18C P_{lac}-*cyaA*$_{T18}$-*mgrB*, Amp^R	[18]
pAL38	pEB52 P_{trc}-*gfpA206K-mgrB*, Amp^R	[18]
pAL39	pEB52 P_{trc}-*gfpA206K*, Amp^R	[18]
pBAD33	*ori*$_{p15A}$ P_{araBAD}-MCS *araC*, Cam^R	ATCC 87402
pCP20	*λcI857(ts) repA101(ts) oriR101 bla cat λpR-FLP*, Amp^R Cam^R	[66]
pEB52	pTrc99a with the NcoI site removed, Amp^R	Goulian lab collection
pJC1	pEB52 P_{trc}-*gfpA206K-mgrB Q30A*, Amp^R	This study
pJC2	pEB52 P_{trc}-*gfpA206K-mgrB D29A*, Amp^R	This study
pJC3	pEB52 P_{trc}-*gfpA206K-mgrB F34A*, Amp^R	This study
pJC4	pEB52 P_{trc}-*gfpA206K-mgrB G37A*, Amp^R	This study
pJC5	pEB52 P_{trc}-*gfpA206K-mgrB I38A*, Amp^R	This study
pJC6	pEB52 P_{trc}-*gfpA206K-mgrB P46A*, Amp^R	This study
pJC7	pEB52 P_{trc}-*gfpA206K-mgrB W47A*, Amp^R	This study
pKD13	*oriR*$_{\gamma R6k}$ *bla FRT::kan::FRT*, Kan^R	[57]
pKD46	*repA101(ts) oriR101 bla ParaB-(gam bet exo)*, Amp^R	[57]
pKK14	pKT25 P_{lac}-*cyaA*$_{T25}$-*envZ*, Kan^R	Goulian lab collection
pKK15	pKT25 P_{lac}-*cyaA*$_{T25}$-*torS*, Kan^R	Goulian lab collection
pKT25	*ori*$_{p15A}$ P_{lac}-*cyaA*$_{T25}$-MCS, Kan^R	Euromedex
pKT25-toxR	pKT25 P_{lac}-*cyaA*$_{T25}$-*Vibrio cholerae toxR*, Kan^R	[67]
pSV1	pEB52 P_{trc}-*gfpA206K-Kp_mgrB*, Amp^R	This study
pSV2	pEB52 P_{trc}-*gfpA206K-Yp_mgrB*, Amp^R	This study
pSV3	pEB52 P_{trc}-*gfpA206K-Pl_mgrB*, Amp^R	This study
pSV4	pEB52 P_{trc}-*gfpA206K-Pp_mgrB*, Amp^R	This study
pSV5	pEB52 P_{trc}-*gfpA206K-Ps_mgrB*, Amp^R	This study
pSV6	pEB52 P_{trc}-*gfpA206K-S sp.MYb239_mgrB*, Amp^R	This study
pSV7	pEB52 P_{trc}-*gfpA206K-El_mgrB*, Amp^R	This study
pSV8	pEB52 P_{trc}-*gfpA206K-St_mgrB*, Amp^R	This study
pSY3	pEB52 P_{trc}-*gfpA206K-mgrB-malF TM swap*, Amp^R	This study
pSY4	pEB52 P_{trc}-*gfpA206K-mgrB-gpA TM swap*, Amp^R	This study
pSY5	pEB52 P_{trc}-*gfpA206K-mgrB-24 (N25->stop)* truncation, Amp^R	This study
pSY6	pEB52 P_{trc}-*gfpA206K-mgrB-29 (Q30->stop)* truncation, Amp^R	This study

pSY7	pEB52 P_{trc}-*gfpA206K-mgrB-34 (F35->stop)* truncation, Amp^R	This study
pSY8	pEB52 P_{trc}-*gfpA206K-mgrB-39 (A40->stop)* truncation, Amp^R	This study
pSY9	pEB52 P_{trc}-*gfpA206K-mgrB-44 (I45->stop)* truncation, Amp^R	This study
pSY29	pEB52 P_{trc}-*gfpA206K-mzrA*, Amp^R	This study
pSY31	pEB52 P_{trc}-*gfpA206K-safA*, Amp^R	This study
pSY32	pEB52 P_{trc}-*gfpA206K-mzrA-gpA TM swap*, Amp^R	This study
pSY33	pEB52 P_{trc}-*gfpA206K-safA-gpA TM swap*, Amp^R	This study
pSY34	pUT18C P_{lac}-*cyaA*$_{T18}$-*mgrB-24* (MgrB truncation mutant lacking periplasmic domain), Amp^R	This study
pSY60	pKT25 P_{lac}-*cyaA*$_{T25}$-*arcB*, Kan^R	This study
pSY61	pKT25 P_{lac}-*cyaA*$_{T25}$-*atoS*, Kan^R	This study
pSY62	pKT25 P_{lac}-*cyaA*$_{T25}$-*baeS*, Kan^R	This study
pSY63	pKT25 P_{lac}-*cyaA*$_{T25}$-*basS*, Kan^R	This study
pSY64	pKT25 P_{lac}-*cyaA*$_{T25}$-*cpxA*, Kan^R	This study
pSY65	pKT25 P_{lac}-*cyaA*$_{T25}$-*cusS*, Kan^R	This study
pSY66	pKT25 P_{lac}-*cyaA*$_{T25}$-*evgS*, Kan^R	This study
pSY67	pKT25 P_{lac}-*cyaA*$_{T25}$-*ntrB*, Kan^R	This study
pSY68	pKT25 P_{lac}-*cyaA*$_{T25}$-*phoR*, Kan^R	This study
pSY69	pKT25 P_{lac}-*cyaA*$_{T25}$-*rstB*, Kan^R	This study
pSY70	pKT25 P_{lac}-*cyaA*$_{T25}$-*qseC*, Kan^R	This study
pSY72	pEB52 P_{trc}-*gfpA206K-mgrB W20A*, Amp^R	This study
pSY73	pEB52 P_{trc}-*gfpA206K-mgrB Q22A*, Amp^R	This study
pSY74	pEB52 P_{trc}-*gfpA206K-mgrB F24A*, Amp^R	This study
pSY75	pEB52 P_{trc}-*gfpA206K-mgrB Q22A N25A*, Amp^R	This study
pTG1	pEB52 P_{trc}-*gfpA206K-mgrB N25A*, Amp^R	This study
pTG2	pEB52 P_{trc}-*gfpA206K-mgrB M26A*, Amp^R	This study
pTG3	pEB52 P_{trc}-*gfpA206K-mgrB I45A*, Amp^R	This study
pTG4	pEB52 P_{trc}-*gfpA206K-mgrB C28A*, Amp^R	This study
pTG5	pEB52 P_{trc}-*gfpA206K-mgrB M27A*, Amp^R	This study
pTG6	pEB52 P_{trc}-*gfpA206K-mgrB D31A*, Amp^R	This study
pTG7	pEB52 P_{trc}-*gfpA206K-mgrB V32A*, Amp^R	This study
pTG8	pEB52 P_{trc}-*gfpA206K-mgrB Q33A*, Amp^R	This study
pTG9	pEB52 P_{trc}-*gfpA206K-mgrB F35A*, Amp^R	This study
pTG10	pEB52 P_{trc}-*gfpA206K-mgrB S36A*, Amp^R	This study
pTG11	pEB52 P_{trc}-*gfpA206K-mgrB C39A*, Amp^R	This study
pTG12	pEB52 P_{trc}-*gfpA206K-mgrB I41A*, Amp^R	This study
pTG13	pEB52 P_{trc}-*gfpA206K-mgrB N42A*, Amp^R	This study
pTG14	pEB52 P_{trc}-*gfpA206K-mgrB Q43A*, Amp^R	This study
pTG15	pEB52 P_{trc}-*gfpA206K-mgrB F44A*, Amp^R	This study
pTrc99a	*lacI*^{q}, P_{trc}-MCS, Amp^R	[68]
pUT18C	pUC19 P_{lac}-*cyaA*$_{T18}$-MCS, Amp^R	Euromedex
pJY31	pUA66 EC P_{mgtLA}-*gfp,* Kan^R	[14]
	pBAD33RBS, Cm^R	[14]
pJY151	pBAD33RBS *mgrB*, Cm^R	This study
pJY501	pBAD33RBS *mgrB K2A*, Cm^R	This study
pJY502	pBAD33RBS *mgrB K3A*, Cm^R	This study
pJY503	pBAD33RBS *mgrB F4A*, Cm^R	This study
pJY504	pBAD33RBS *mgrB R5A*, Cm^R	This study
pJY505	pBAD33RBS *mgrB W6A*, Cm^R	This study
pJY506	pBAD33RBS *mgrB C16A*, Cm^R	This study
pJY507	pBAD33RBS *mgrB W20A*, Cm^R	This study
pJY508	pBAD33RBS *mgrB Q22A*, Cm^R	This study
pJY509	pBAD33RBS *mgrB F24A*, Cm^R	This study

pJY510	pBAD33RBS *mgrB N25A*, Cm^R	This study
pJY511	pBAD33RBS *mgrB M26A*, Cm^R	This study
pJY512	pBAD33RBS *mgrB M27A*, Cm^R	This study
pJY513	pBAD33RBS *mgrB C28A*, Cm^R	This study
pJY514	pBAD33RBS *mgrB D29A*, Cm^R	This study
pJY515	pBAD33RBS *mgrB D31A*, Cm^R	This study
pJY516	pBAD33RBS *mgrB V32A*, Cm^R	This study
pJY517	pBAD33RBS *mgrB F34A*, Cm^R	This study
pJY518	pBAD33RBS *mgrB F35A*, Cm^R	This study
pJY519	pBAD33RBS *mgrB I38A*, Cm^R	This study
pJY520	pBAD33RBS *mgrB C39A*, Cm^R	This study
pJY521	pBAD33RBS *mgrB I41A*, Cm^R	This study
pJY522	pBAD33RBS *mgrB F44A*, Cm^R	This study
pJY523	pBAD33RBS *mgrB I45A*, Cm^R	This study
pJY524	pBAD33RBS *mgrB W47A*, Cm^R	This study
pJY525	pBAD33RBS *mgrB K2R*, Cm^R	This study
pJY526	pBAD33RBS *mgrB K2H*, Cm^R	This study
pJY527	pBAD33RBS *mgrB K2D*, Cm^R	This study
pJY528	pBAD33RBS *mgrB K2E*, Cm^R	This study
pJY529	pBAD33RBS *mgrB K2S*, Cm^R	This study
pJY530	pBAD33RBS *mgrB K2T*, Cm^R	This study
pJY531	pBAD33RBS *mgrB K2N*, Cm^R	This study
pJY532	pBAD33RBS *mgrB K2Q*, Cm^R	This study
pJY533	pBAD33RBS *mgrB K2C*, Cm^R	This study
pJY534	pBAD33RBS *mgrB K2P*, Cm^R	This study
pJY535	pBAD33RBS *mgrB K2G*, Cm^R	This study
pJY536	pBAD33RBS *mgrB K2V*, Cm^R	This study
pJY537	pBAD33RBS *mgrB K2L*, Cm^R	This study
pJY538	pBAD33RBS *mgrB K2I*, Cm^R	This study
pJY539	pBAD33RBS *mgrB K2M*, Cm^R	This study
pJY540	pBAD33RBS *mgrB K2F*, Cm^R	This study
pJY541	pBAD33RBS *mgrB K2Y*, Cm^R	This study
pJY542	pBAD33RBS *mgrB K2W*, Cm^R	This study
pJY543	pBAD33RBS *mgrB K3R*, Cm^R	This study
pJY544	pBAD33RBS *mgrB K3H*, Cm^R	This study
pJY545	pBAD33RBS *mgrB K3D*, Cm^R	This study
pJY546	pBAD33RBS *mgrB K3E*, Cm^R	This study
pJY547	pBAD33RBS *mgrB K3S*, Cm^R	This study
pJY548	pBAD33RBS *mgrB K3T*, Cm^R	This study
pJY549	pBAD33RBS *mgrB K3N*, Cm^R	This study
pJY550	pBAD33RBS *mgrB K3Q*, Cm^R	This study
pJY551	pBAD33RBS *mgrB K3C*, Cm^R	This study
pJY552	pBAD33RBS *mgrB K3P*, Cm^R	This study
pJY553	pBAD33RBS *mgrB K3G*, Cm^R	This study
pJY554	pBAD33RBS *mgrB K3V*, Cm^R	This study
pJY555	pBAD33RBS *mgrB K3L*, Cm^R	This study
pJY556	pBAD33RBS *mgrB K3I*, Cm^R	This study
pJY557	pBAD33RBS *mgrB K3M*, Cm^R	This study
pJY558	pBAD33RBS *mgrB K3F*, Cm^R	This study
pJY559	pBAD33RBS *mgrB K3Y*, Cm^R	This study
pJY560	pBAD33RBS *mgrB K3W*, Cm^R	This study
pJY561	pBAD33RBS *mgrB K2DK3D*, Cm^R	This study
pJY562	pBAD33RBS *mgrB K2HK3H*, Cm^R	This study

pJY563	pBAD33RBS *mgrB K2RK3R*, Cm^R	This study
pJY564	pBAD33RBS *flag*-flexilinker-*mgrB*, Cm^R	This study
pJY565	pBAD33RBS *flag*-flexilinker-*mgrB K2A*, Cm^R	This study
pJY566	pBAD33RBS *flag*-flexilinker-*mgrB K3A*, Cm^R	This study
pJY567	pBAD33RBS *flag*-flexilinker-*mgrB K2DK3D*, Cm^R	This study
pOB2	pTrc99A *mcherry,* Amp^R	[60]
pJY569	pTrc99A *mcherry-mgrB,* Amp^R	This study
pJY570	pTrc99A *mcherry-mgrB K2A,* Amp^R	This study
pJY571	pTrc99A *mcherry-mgrB K3A,* Amp^R	This study
pJY572	pTrc99A *mcherry-mgrB K2DK3D,* Amp^R	This study
pJY573	pBAD33RBS *phoQ-mneongreen*	This study

921
922 **S3 Table. Primers**
923

Primer	**Sequence (5' -> 3')**	**Use**
atoS-xbaI-U1	ACTCTAGAGATGCATTATATGAAGTGGATTTATC	Cloning of *cyaA*$_{T25}$-*atoS*
atoS-kpnI-L1	CATGGTACCCAGTCATACAGTCTGATTTCCCTG	
b1500-red-u1	ACTGATTAACGATTTTTAACGTTATCCGCTAAATAAACATATTTGAAATGATTCCGGGGATCCGTCGACC	Generation of Δ*safA*::(*FRT-kan-FRT*)
b1500-red-l1	ATTTCATATTTATAATTTGCTGTTTGTTTTCAGCCTTGCAAACTATTGATTGTAGGCTGGAGCTGCTTCG	
cpxA-xbaI-U1	ACTCTAGAGATGATAGGCAGCTTAACCG	Cloning of *cyaA*$_{T25}$-*cpxA*
cpxA-kpnI-L1	CATGGTACCCCTGCAAATGCGAAGTTTAACTC	
gfp-Cterm-L1	TTTGTATAGTTCATCCATGCCATGTGTAATCCCAG	Cloning of *gfpA206K-mzrA, -safA*
gfp-mzrA-U1	ACATGGCATGGATGAACTATACAAAATGCAAATACCTCGCATGTCGCTTC	Cloning of *gfpA206K-mzrA*
gfp-safA-U1	ACATGGCATGGATGAACTATACAAAATGCATGCGACCACAGTGAAAAACAAAATC	Cloning of *gfpA206K-safA*
GpA-TM-U1	GTGATTGGCACCATTCTGCTGATTAGCTATAACATGATGTGCGATCAGGATG	Cloning of *gfpA206K-mgrB-gpA TM swap*
GpA-TM-L1	GCCCGCCATCACGCCAAAAATAATCGCGGTAATCCATCGAAACTTTTTCATTTTGTATAG	
MalF-TM-U1	GTGGGTTACCTTGTTGTTTTAATGTACGCAAACATGATGTGCGATCAGGATG	Cloning of *gfpA206K-mgrB-malF TM swap*
MalF-TM-L1	CAGCAGGCCGAGCAGACCTAGCACTGACCACCATCGAAACTTTTTCATTTTGTATAG	
mgrB_stop-pAL38-U1	TGAACTAGAGTCGACCTGCAG	Cloning of *gfpA206K-mgrB-24*, *mgrB-29*, *mgrB-34*, *mgrB-39 and mgrB-44*
mgrB-N25stop-L1	GAATACCTGCGCCCAAAGC	Cloning of *gfpA206K-mgrB-24*, and T18-*mgrB*
mgrB-Q30stop-L1	ATCGCACATCATGTTGAATACCTG	Cloning of *gfpA206K-mgrB-29*

mgrB-F35stop-L1	AAATTGTACATCCTGATCGCACATC	Cloning of *gfpA206K-mgrB-34*
mgrB-A40stop-L1	ACAAATTCCGCTGAAAAATTGTACATCC	Cloning of *gfpA206K-mgrB-39*
mgrB-I45stop-L1	AAACTGGTTAATGGCACAAATTCCGC	Cloning of *gfpA206K-mgrB-44*
mgrB_stop-pAL33-U1	TGAATAAGTAGGGTACCGAGCTC	Cloning of T18-*mgrB*
mgrB W20A-U1	GCGCAGGTATTCAACATGATGTGC	Construction of *gfpA206K-mgrB W20A* in pAL38 by site-directed mutagenesis
mgrB W20A-L1	CGCAAGCAGCAAGCAAGCCAACAC	
mgrB Q22A-U1	GTATTCAACATGATGTGCGATCAGGATG	Construction of *gfpA206K-mgrB Q22A* in pAL38 by site-directed mutagenesis
mgrB Q22A-L1	CGCCGCCCAAAGCAGCAAGCAAGC	
mgrB F24A-U1	AACATGATGTGCGATCAGGATGTAC	Construction of *gfpA206K-mgrB F24A* in pAL38 by site-directed mutagenesis
mgrB F24A-L1	CGCTACCTGCGCCCAAAGCAGCAAG	
mgrB-N25A-U2	ATGATGTGCGATCAGGATGTAC	Cloning of *gfpA206K-mgrB N25A* in pAL38 by site-directed mutagenesis
mgrB-N25A-L2	CGCGAATACCTGCGCCCAAAGC	
mgrB_M26A_U1	GCGCAGGTATTCAACGCGATGTGCGATCAGGATG	Construction of *gfpA206K-mgrB M26A* in pAL38 by site-directed mutagenesis
mgrB_M26A_L1	CATCCTGATCGCACATCGCGTTGAATACCTGCGC	
mgrB_M27A_U1	GCAGGTATTCAACATGGCGTGCGATCAGGATGTAC	Construction of *gfpA206K-mgrB M27A* in pAL38 by site-directed mutagenesis
mgrB_M27A_L1	GTACATCCTGATCGCACGCCATGTTGAATACCTG	
mgrB_C28A_U1	AGGTATTCAACATGATGGCCGATCAGGATGTACAATTTTTC	Construction of *gfpA206K-mgrB C28A* in pAL38 by site-directed mutagenesis
mgrB_C28A_L1	AATTGTACATCCTGATCGGCCATCATGTTGAATACCT	
mgrB_D29A	AGGTATTCAACATGATGTGCGCTCAGGATGTACAATTTTTCAG	Construction of *gfpA206K-mgrB D29A* in pAL38 by site-directed mutagenesis
mgrB_D29A_as	CTGAAAAATTGTACATCCTGAGCGCACATCATGTTGAATACCT	
mgrB_Q30A	AGGTATTCAACATGATGTGCGATGCGGATGTACAATTTTTCAGCG	Construction of *gfpA206K-mgrB Q30A* in pAL38 by site-directed mutagenesis
mgrB_Q30A_as	CGCTGAAAAATTGTACATCCGCATCGCACATCATGTTGAATACCT	

mgrB_D31A_U1	ACATGATGTGCGATCAGGCGGTACAATTTTTCAGCGG	Construction of *gfpA206K-mgrB D31A* in pAL38 by site-directed mutagenesis
mgrB_D31A_L1	CCGCTGAAAAATTGTACCGCCTGATCGCACATCATGT	
mgrB_V32A_U1	TGATGTGCGATCAGGATGCGCAATTTTTCAGCGGAATTTG	Construction of *gfpA206K-mgrB V32A* in pAL38 by site-directed mutagenesis
mgrB_V32A_L1	ATTCCGCTGAAAAATTGCGCATCCTGATCGCACATC	
mgrB_Q33A_U1	TGTGCGATCAGGATGTAGCATTTTTCAGCGGAATTTG	Construction of *gfpA206K-mgrB Q33A* in pAL38 by site-directed mutagenesis
mgrB_Q33A_L1	CAAATTCCGCTGAAAAATGCTACATCCTGATCGCAC	
mgrB_F34A	GTGCGATCAGGATGTACAAGCTTTCAGCGGAATTTGTGCC	Construction of *gfpA206K-mgrB F34A* in pAL38 by site-directed mutagenesis
mgrB_F34A_as	GGCACAAATTCCGCTGAAAGCTTGTACATCCTGATCGCAC	
mgrB_F35A_U1	TCAGGATGTACAATTTGCCAGCGGAATTTGTGCC	Construction of *gfpA206K-mgrB F35A* in pAL38 by site-directed mutagenesis
mgrB_F35A_L1	TGGCACAAATTCCGCTGGCAAATTGTACATCCTG	
mgrB_S36A_U1	GATGTACAATTTTTCGCCGGAATTTGTGCCATTAAC	Construction of *gfpA206K-mgrB S36A* in pAL38 by site-directed mutagenesis
mgrB_S36A_L1	AATGGCACAAATTCCGGCGAAAAATTGTACATCC	
mgrB_G37A	GGATGTACAATTTTTCAGCGCAATTTGTGCCATTAACCAGT	Construction of *gfpA206K-mgrB G37A* in pAL38 by site-directed mutagenesis
mgrB_G37A_as	ACTGGTTAATGGCACAAATTGCGCTGAAAAATTGTACATCC	
mgrB_I38A	AGGATGTACAATTTTTCAGCGGAGCTTGTGCCATTAACCAGTTTATCC	Construction of *gfpA206K-mgrB I38A* in pAL38 by site-directed mutagenesis
mgrB_I38A_as	GGATAAACTGGTTAATGGCACAAGCTCCGCTGAAAAATTGTACATCCT	
mgrB_C39A_U1	AATTTTTCAGCGGAATTGCTGCCATTAACCAGTTTAT	Construction of *gfpA206K-mgrB C39A* in pAL38 by site-directed mutagenesis
mgrB_C39A_L1	ATAAACTGGTTAATGGCAGCAATTCCGCTGAAAAATTG	
mgrB_I41A_U1	TCAGCGGAATTTGTGCCGCTAACCAGTTTATCCCG	Construction of *gfpA206K-mgrB I41A* in pAL38 by site-directed mutagenesis
mgrB_I41A_L1	ACGGGATAAACTGGTTAGCGGCACAAATTCCGCTG	
mgrB_N42A_U1	GGAATTTGTGCCATTGCCCAGTTTATCCCGTGG	Construction of *gfpA206K-mgrB N42A* in

mgrB_N42A_L1	CCACGGGATAAACTGGGCAATGGCACAAATTCC	pAL38 by site-directed mutagenesis
mgrB_Q43A_U1	GAATTTGTGCCATTAACGCGTTTATCCCGTGGTGAAC	Construction of *gfpA206K-mgrB Q43A* in pAL38 by site-directed mutagenesis
mgrB_Q43A_L1	GTTCACCACGGGATAAACGCGTTAATGGCACAAATTC	
mgrB_F44A_U1	ATTTGTGCCATTAACCAGGCTATCCCGTGGTGAACTAGAG	Construction of *gfpA206K-mgrB F44A* in pAL38 by site-directed mutagenesis
mgrB_F44A_L1	TCTAGTTCACCACGGGATAGCCTGGTTAATGGCACAAATTC	
mgrB-I45A-U2	CCGTGGTGAACTAGAGTCGAC	Construction of *gfpA206K-mgrB I45A* in pAL38 by site-directed mutagenesis
mgrB-I45A-L2	CGCAAACTGGTTAATGGCACAAATTCC	
mgrB(pAL38)_P46A	GCCATTAACCAGTTTATCGCGTGGTGAACTAGAGTC	Construction of *gfpA206K-mgrB P46A* in pAL38 by site-directed mutagenesis
mgrB(pAL38)_P46A_as	GACTCTAGTTCACCACGCGATAAACTGGTTAATGGC	
mgrB(pAL38)_W47A	CATTAACCAGTTTATCCCGGCGTGAACTAGAGTCGACCTG	Construction of *gfpA206K-mgrB W47A* in pAL38 by site-directed mutagenesis
mgrB(pAL38)_W47A_as	CAGGTCGACTCTAGTTCACGCCGGGATAAACTGGTTAATG	
mzrA-GpA-TM-U1	GTGATTGGCACCATTCTGCTGATTAGCTATCGCCAGCAAGAGTCTACGCTG	Cloning of *gfpA206K-mzrA-gpA TM swap*
mzrA-GpA-TM-L1	GCCCGCCATCACGCCAAAAATAATCGCGGTAATCTGGCGAAGCGACATGCGAG	
pEB52-U1	ACTAGAGTCGACCTGCAGGCATGCAAG	Cloning of *gfpA206K-mzrA, -safA*
pEB52-L1	GGGTACCGAGCTCGAATTCTCTGTTTC	
pEB52-gfp-U1	AACAGAGAATTCGAGCTCGGTACCC	
pEB52-mzrA-L1	TGCATGCCTGCAGGTCGACTCTAGTTTATCCGAAGCGATGAGAGTTATCCC	Cloning of *gfpA206K-mzrA*
pEB52-safA-L1	TGCATGCCTGCAGGTCGACTCTAGTTCAGCCTTGCAAACTATTGATAATGAAATGTG	Cloning of *gfpA206K-safA*
phoR-xbaI-U2	ACTCTAGAGATGCTGGAACGGCTGTCGTG	Cloning of *cyaA*$_{T25}$*-phoR*
phoR-kpnI-L1	TGGCTGGTACCGATGACAAAGGCGGATTAATC	
safA-GpA-TM-U1	GTGATTGGCACCATTCTGCTGATTAGCTATATTGATCAGCTGAGTATTTCAGAAATGG	Cloning of *gfpA206K-safA-gpA TM swap*
safA-GpA-TM-L1	GCCCGCCATCACGCCAAAAATAATCGCGGTAATTTCTTTATAGTTGTCTCTTTGCGTGATTTTGTTTTTC	
MgrB K2A fw	CGAGCTCATGGCGAAGTTTCGATGGGTC	Construction of *mgrB K2A* by mutagenesis
MgrB K2A rv	AACTCCTCGCTAGCCCAA	
MgrB K3A fw	GCTCATGAAAGCGTTTCGATGGGTCGTTC	Construction of *mgrB K3A* by mutagenesis
MgrB K3A rv	TCGAACTCCTCGCTAGCC	
MgrB F4A fw	CATGAAAAAGGCGCGATGGGTCGTTCTG	Construction of *mgrB*

MgrB F4A rv	AGCTCGAACTCCTCGCTA	*F4A* by mutagenesis
MgrB R5A fw	GAAAAAGTTTGCGTGGGTCGTTCTGGTTGTC	Construction of *mgrB R5A* by mutagenesis
MgrB R5A rv	ATGAGCTCGAACTCCTCG	
MgrB W6A fw	AAAGTTTCGAGCGGTCGTTCTGGTTG	Construction of *mgrB W6A* by mutagenesis
MgrB W6A rv	TTCATGAGCTCGAACTCC	
MgrB W20A fw	CTTGCTGCTTGCGGCGCAGGTATTC	Construction of *mgrB W20A* in pJY151 by mutagenesis
MgrB W20A rv	CAAGCCAACACCACGACA	
MgrB F24A fw	GGCGCAGGTAGCGAACATGATGTGC	Construction of *mgrB F24A* in pJY151 by mutagenesis
MgrB F24A rv	CAAAGCAGCAAGCAAGCC	
MgrB M26A fw	GGTATTCAACGCGATGTGCGATCAGGATGTACAATTTTTC	Construction of *mgrB M26A* in pJY151 by mutagenesis
MgrB M26A rv	TGCGCCCAAAGCAGCAAG	
MgrB M27A fw	ATTCAACATGGCGTGCGATCAGGATGTACAATTTTTCAGC	Construction of *mgrB M27A* in pJY151 by mutagenesis
MgrB M27A rv	ACCTGCGCCCAAAGCAGC	
MgrB C28A fw	CAACATGATGGCCGATCAGGATGTACAATTTTTC	Construction of *mgrB C28A* in pJY151 by mutagenesis
MgrB C28A rv	AATACCTGCGCCCAAAGC	
MgrB D29A fw	CATGATGTGCGCGCAGGATGTACAATTTTTC	Construction of *mgrB D29A* in pJY151 by mutagenesis
MgrB D29A rv	TTGAATACCTGCGCCCAA	
MgrB D31A fw	GTGCGATCAGGCGGTACAATTTTTC	Construction of *mgrB D31A* in pJY151 by mutagenesis
MgrB D31A rv	ATCATGTTGAATACCTGC	
MgrB V32A fw	GATCAGGATGCGCAATTTTTCAGCG	Construction of *mgrB V32A* in pJY151 by mutagenesis
MgrB V32A rv	GCACATCATGTTGAATAC	
MgrBF34A fw	GGATGTACAAGCGTTCAGCGGAATTTG	Construction of *mgrB F34A* in pJY151 by mutagenesis
MgrB F34A rv	TGATCGCACATCATGTTG	
MgrB F35A fw	TGTACAATTTGCGAGCGGAATTTGTG	Construction of *mgrB F35A* in pJY151 by mutagenesis
MgrB F35A rv	TCCTGATCGCACATCATG	
MgrB I38A fw	TTTCAGCGGAGCGTGTGCCATTAAC	Construction of *mgrB I38A* in pJY151 by mutagenesis
MgrB I38A rv	AATTGTACATCCTGATCG	
MgrB C39A fw	CAGCGGAATTGCCGCCATTAACC	Construction of *mgrB C39A* in pJY151 by mutagenesis
MgrB C39A rv	AAAAATTGTACATCCTGATCG	
MgrB I41A fw	AATTTGTGCCGCGAACCAGTTTATCC	Construction of *mgrB I41A* in pJY151 by mutagenesis
MgrB I41A rv	CCGCTGAAAAATTGTACATC	
MgrB F44A fw	CATTAACCAGGCGATCCCGTGGTG	Construction of *mgrB F44A* in pJY151 by mutagenesis
MgrB F44A rv	GCACAAATTCCGCTGAAAAATTG	
MgrB I45A fw	TAACCAGTTTGCGCCGTGGTGATCTAG	Construction of *mgrB I45A* in pJY151 by mutagenesis
MgrB I45A rv	ATGGCACAAATTCCGCTG	
MgrB W47A fw	GTTTATCCCGGCGTGATCTAGAGTC	Construction of *mgrB W47A* in pJY151 by mutagenesis
MgrB W47A rv	TGGTTAATGGCACAAATTC	

MgrB K2R fw	CGAGCTCATGCGTAAGTTTCGATGGGTC	Construction of *mgrB K2X* in pBAD33RBS vector by site-directed mutagenesis
MgrB K2H fw	CGAGCTCATGCATAAGTTTCGATGGGTC	
MgrB K2D fw	CGAGCTCATGGATAAGTTTCGATGGG	
MgrB K2E fw	CGAGCTCATGGAAAAGTTTCGATG	
MgrB K2S fw	CGAGCTCATGAGCAAGTTTCGATGGG	
MgrB K2T fw	CGAGCTCATGACCAAGTTTCGATGGGTCG	
MgrB K2N fw	CGAGCTCATGAACAAGTTTCGATGG	
MgrB K2Q fw	CGAGCTCATGCAGAAGTTTCGATGGG	
MgrB K2C fw	CGAGCTCATGTGCAAGTTTCGATGGGTC	
MgrB K2P fw	CGAGCTCATGCCGAAGTTTCGATGGGTC	
MgrB K2G fw	CGAGCTCATGGGCAAGTTTCGATGGGTC	
MgrB K2V fw	CGAGCTCATGGTGAAGTTTCGATGGGTC	
MgrB K2L fw	CGAGCTCATGCTGAAGTTTCGATGGGTC	
MgrB K2I fw	CGAGCTCATGATTAAGTTTCGATGGGTC	
MgrB K2M fw	CGAGCTCATGATGAAGTTTCGATGGG	
MgrB K2F fw	CGAGCTCATGTTTAAGTTTCGATGGGTCG	
MgrB K2Y fw	CGAGCTCATGTATAAGTTTCGATGGGTC	
MgrB K2W fw	CGAGCTCATGTGGAAGTTTCGATGGGTC	
MgrB K3R fw	GCTCATGAAACGTTTTCGATGGGTCGTTCTGGTTGTC	Construction of *mgrB K3X* in pBAD33RBS vector by site-directed by mutagenesis
MgrB K3H fw	GCTCATGAAACATTTTCGATGGGTCGTTC	
MgrB K3D fw	GCTCATGAAAGATTTTCGATGGGTCGTTC	
MgrB K3E fw	GCTCATGAAAGAATTTCGATGGGTCG	
MgrB K3S fw	GCTCATGAAAAGCTTTCGATGGGTCGTTCTGGTTG	
MgrB K3T fw	GCTCATGAAAACCTTTCGATGGGTCGTTCTGGTTGTC	
MgrB K3N fw	GCTCATGAAAAACTTTCGATGGGTCGTTC	
MgrB K3Q fw	GCTCATGAAACAGTTTCGATGGGTC	
MgrB K3C fw	GCTCATGAAATGCTTTCGATGGGTCGTTCTGGTTGTC	
MgrB K3P fw	GCTCATGAAACCGTTTCGATGGGTCGTTCTGG	
MgrB K3G fw	GCTCATGAAAGGCTTTCGATGGGTCGTTCTGGTTG	
MgrB K3V fw	GCTCATGAAAGTGTTTCGATGGGTCGTTC	
MgrB K3L fw	GCTCATGAAACTGTTTCGATGGGTCGTTCTGG	
MgrB K3I fw	GCTCATGAAAATTTTTCGATGGGTCGTTCTGGTTG	
MgrB K3M fw	GCTCATGAAAATGTTTCGATGGGTC	
MgrB K3F fw	GCTCATGAAATTTTTTCGATGGGTCGTTCTGGTTGTC	
MgrB K3Y fw	GCTCATGAAATATTTTCGATGGGTCGTTCTG	
MgrB K3W fw	GCTCATGAAATGGTTTCGATGGGTCGTTCTG	
MgrB K2DK3D fw	CGAGCTCATGGATGATTTTCGATGGGTCGTTC	Construction of *mgrB K2DK3D* by mutagenesis

MgrB K2RK3R fw	CGAGCTCATGCGTCGTTTTCGATGGGTC GTTCTGG	Construction of *mgrB K2RK3R* by mutagenesis
MgrB K2HK3H fw	CGAGCTCATGCATCATTTTCGATGGGTCG TTCTG	Construction of *mgrB K2HK3H* by mutagenesis
MgrB K2K3 rv	AACTCCTCGCTAGCCCAA	Construction of *mgrB K2XK3X* by mutagenesis
PhoQ TM2 fw	GAGCTAAAAAGTTCCTATATGGTC GAG CTA AAA AGT TCC TAT ATG GTC	Construction of PhoQ TM2-HAMP region random mutagenesis library
PhoQ HAMP rv	GGTGAGCGTCGTACGGTATTT	
PhoQ R219Dfw	GTGGAGTTTAgatCCCATCGAAGCCCTGGCAAA AGAAGTCCG	Construction of PhoQ R219X mutants by site-directed mutagenesis
PhoQ R219rv	CAGGCGGCGACCCACAGC	
PhoQ R219Efw	GTGGAGTTTAgaaCCCATCGAAGCCCTGGCAAA AGAAGTCCG	
PhoQ R219Nfw	GTGGAGTTTAaacCCCATCGAAGCCCTGGCAAA AGAAG	
PhoQ R219Qfw	GTGGAGTTTAcagCCCATCGAAGCCCTGGCAAA AG	

924

925 **Supplementary Figures**

926

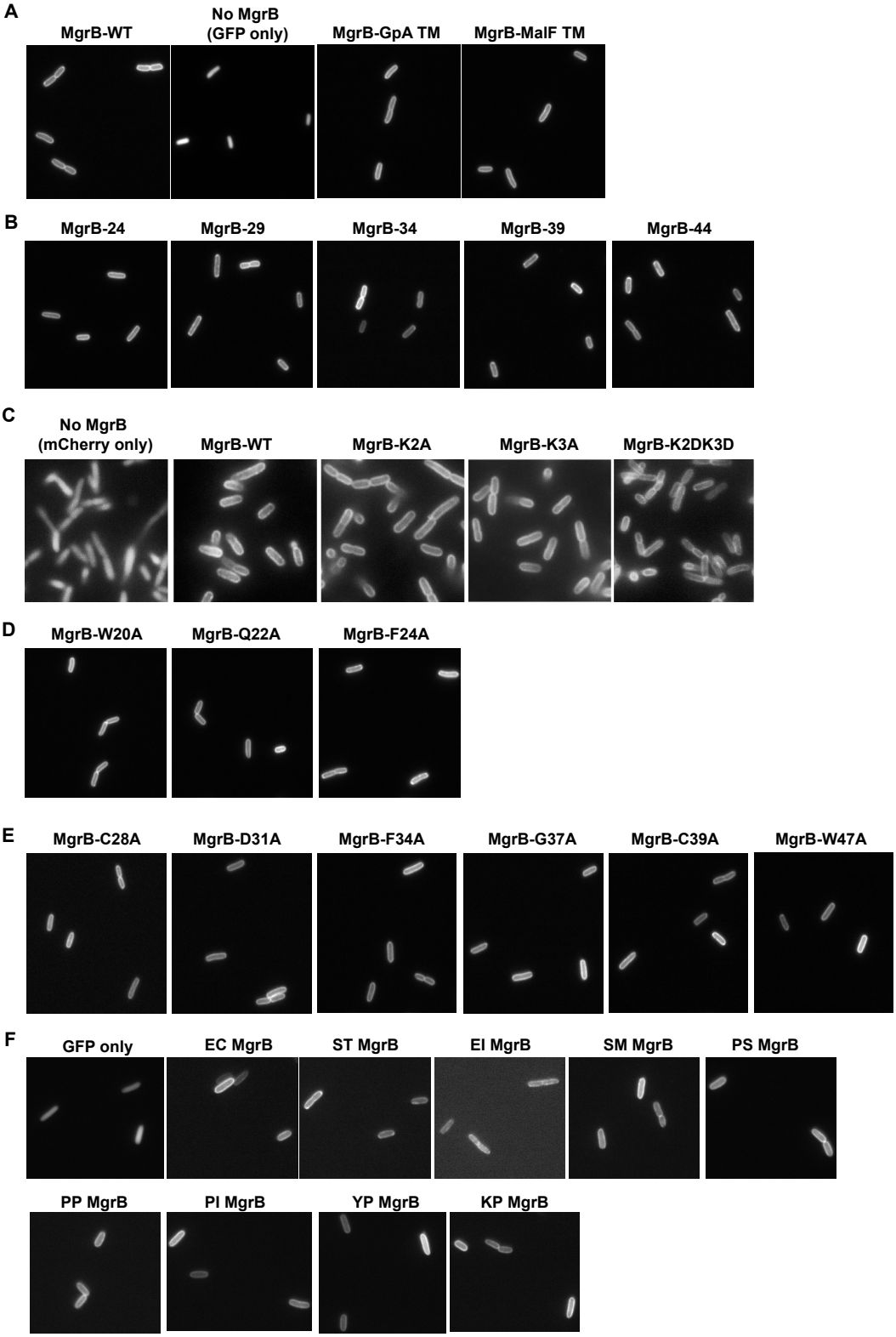

927

928

929 **S1 Fig.** Visualization of cellular localization of MgrB and its variants by microscopy. **A**,
930 Representative fluorescence microscopy images of cells expressing wild-type MgrB, GFP-
931 only, and MgrB variants where the transmembrane region is swapped with transmembrane
932 domain from either human GpA or MalF, respectively. **B**, Representative green fluorescence
933 images of cells expressing C-terminal truncations of MgrB – MgrB-24 (TM only construct, no
934 periplasmic domain), MgrB-29, MgrB-34, MgrB-39 and MgrB-44. **C**, Representative
935 fluorescence microscopy images of cells expressing mCherry-only, mCherry tagged wild-
936 type MgrB and MgrB variants with indicated mutations. **D**, Representative green
937 fluorescence images of cells expressing TM region single Ala mutants of MgrB – W20A,
938 Q22A and F24A. **E**, Representative green fluorescence images of cells expressing
939 periplasmic single Ala mutants of MgrB – C28A, D31A, F34A, G37A, C39A and W47A. *E.*
940 *coli* MG1655 with *mgrB* deletion is the strain background in C and AML67 is the strain
941 background in A, B, D and E. **F**, Representative green fluorescence images of cells
942 expressing MgrB orthologs (EC- *E. coli*, ST- *Salmonella enterica serovar typhimurium*, EL-
943 *Enterobacter ludwigii*, SM- *Serratia sp.MYb239*, PS- *Providencia stuartii*, PP- *Proteus*
944 *penneri*, PL- *Photorhabdus laumondii*, YP- *Yesinia pestis* and KP- *Klebsiella pneumoniae*).
945 Inducer was not added as the leaky expression from the *trc* promoter resulted in sufficient
946 levels of protein except for constructs in panel C, where 10 μM IPTG was added.
947
948

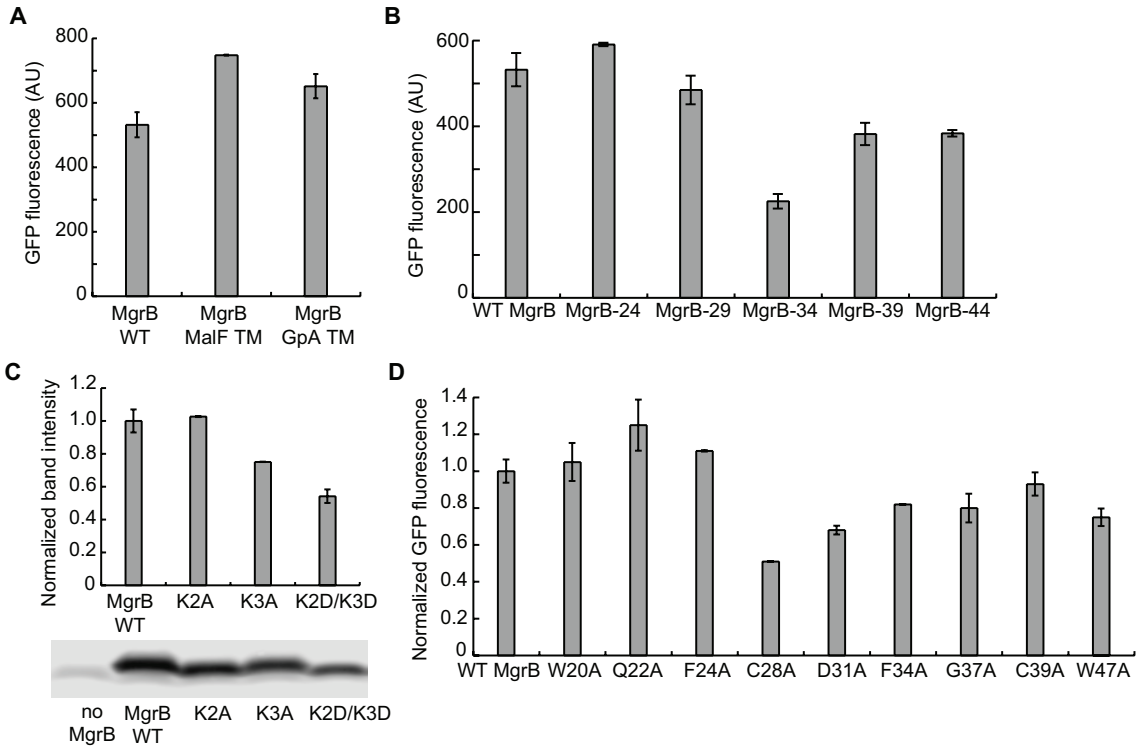

S2 Fig. GFP-MgrB expression levels for MgrB variants relative to wild type. GFP-MgrB expression levels for cells expressing (**A**) MgrB TM hybrids, (**B**) MgrB truncation mutants and (**D**) the site-directed single alanine mutants were imaged by fluorescence microscopy and GFP fluorescence levels were quantified (see Methods for details). Data represent averages and ranges for two independent experiments comprised of at least 50 cells each, AU = Arbitrary Units. **C**, The expression level of the FLAG tagged wild-type and MgrB mutants were monitored by western blot. A representative western blot is below. The band intensities were quantified using ImageJ and normalized to wild-type MgrB after taking account of total protein amount in each sample. Data represent averages of three independent experiments and error bars show SDs.

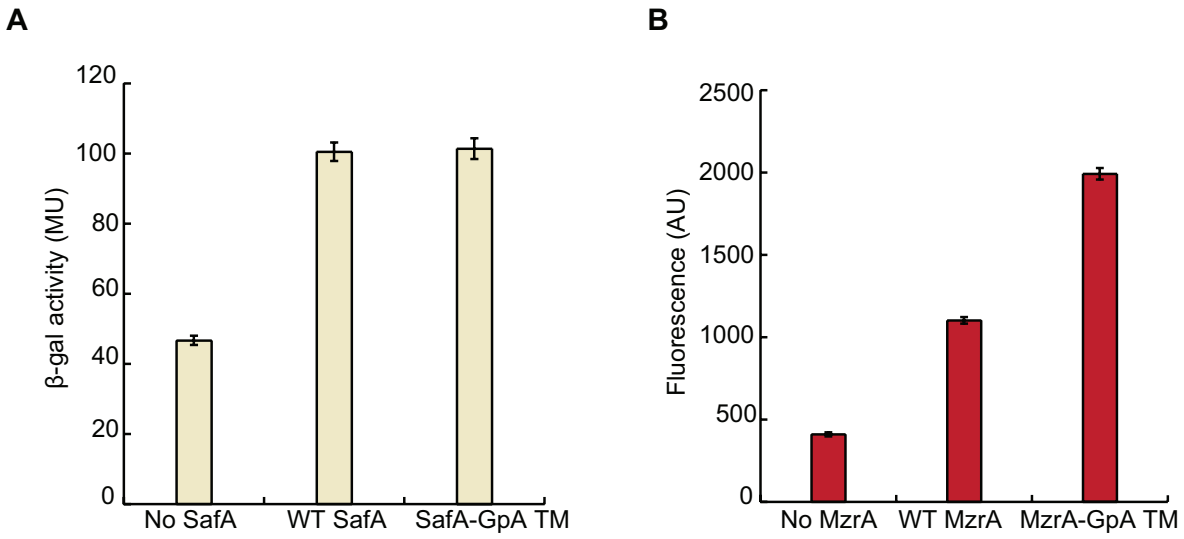

963
964
965 **S3 Fig. Transmembrane sequences of histidine kinase regulators, SafA and MzrA, are**
966 **dispensable for their function.**
967 **A**, Activities of wild-type SafA and its variant where the transmembrane region is swapped
968 with transmembrane domain from human glycophorin A (GpA) measured as a function of β-
969 galactosidase levels in a Δ*safA* strain containing PhoQ/PhoP-regulated transcriptional
970 reporter P_{mgtA}-*lacZ* (SAM76), MU = Miller Units. **B**, Activities of wild-type MzrA and its variant
971 where the transmembrane region is swapped with transmembrane domain from human GpA
972 measured as a function of red fluorescence levels in a Δ*mzrA* strain containing EnvZ/OmpR-
973 regulated transcriptional reporter P_{ompC}-*mCherry* (SAM72), AU = Arbitrary Units. Inducer
974 (IPTG) was not added as the leaky expression from the *trc* promoter resulted in sufficient
975 levels of protein. Data represent averages and ranges for two independent experiments.
976
977

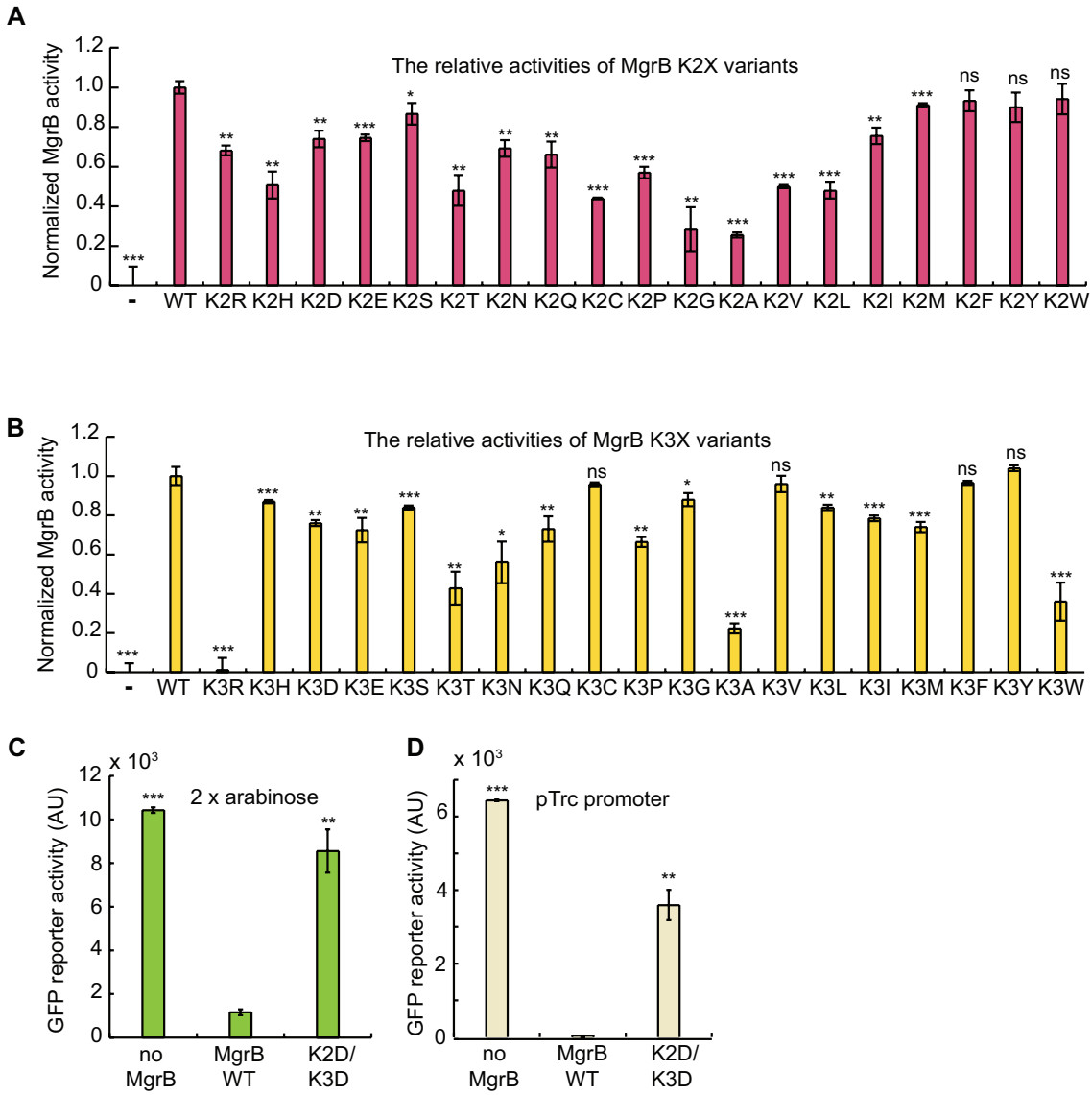

S4 Fig. **The activities of MgrB variants with mutations in the cytosolic region.** The normalized activities of MgrB mutants with single alanine substitutions at K2 (**A**) and K3 (**B**) were tested using the PhoQ/PhoP-regulated transcriptional reporter P_{mgtLA}-*gfp* in a Δ*mgrB* strain (see Materials and methods for the definition of normalized activity). MgrB mutants were constructed in a pBAD33 vector and their expression was induced with 0.008% arabinose. The activities of MgrB K2DK3D were tested as in **A** but with double the amount of arabinose inducer (0.016%) (**C**) or with a different plasmid expression construct (**D**). Specifically, in **D**, MgrB variants were expressed from the basal activity of the *trc* promoter (i.e. without inducer) in the plasmid pTrc99a. Mutants with normalized MgrB activity less than 0.4 were selected for further analysis. Data points represent averages of at least three independent experiments and error bars show SDs. The statistical significances of changes in reporter activity or normalized MgrB activity were calculated with *t* tests by comparing to wild type and indicated with asterisks (*** $P \leq 0.001$, ** $P \leq 0.01$, * $P \leq 0.05$, ns = not significant).

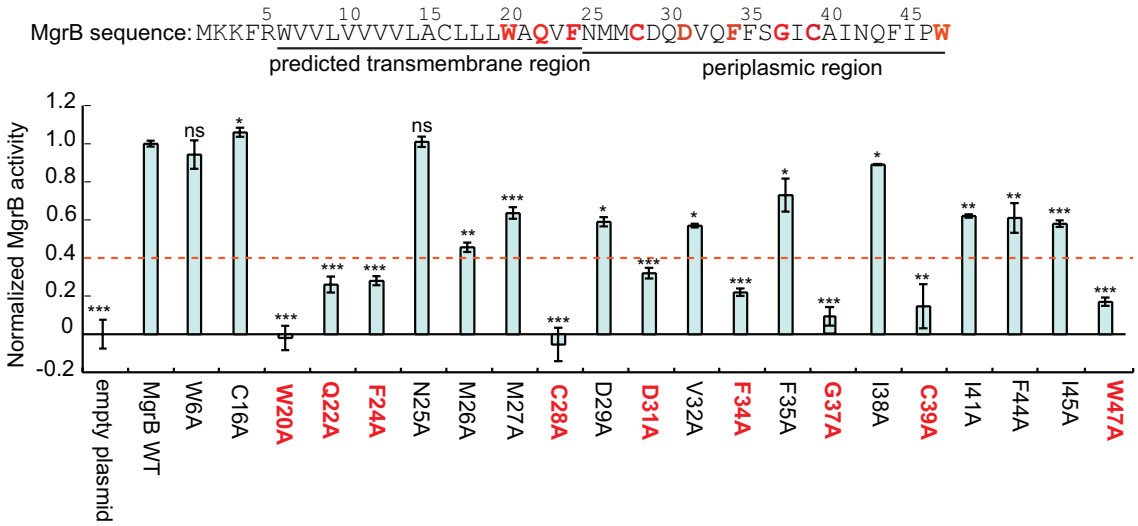

S5 Fig. The normalized activities of MgrB variants with alanine substitutions at indicated positions.

The activities of MgrB mutants with single alanine substitution were tested using PhoQ/PhoP-regulated transcriptional reporter P_{mgtLA}-*gfp* in a Δ*mgrB* strain. MgrB mutants were constructed in a pBAD33 vector and their expression was induced with 0.008% arabinose. The normalized activity was calculated and plotted (see Materials and methods for the definition of normalized activity). Mutants with normalized MgrB activity less than 0.4 (as indicated by the red dashed line) were selected for further analysis. All data points represent averages of at least three independent experiments and error bars show SDs. The statistical significances of changes in normalized MgrB activity were calculated with *t* tests by comparing to wild type and indicated with asterisks (*** $P \leq 0.001$, ** $P \leq 0.01$, * $P \leq 0.05$, ns = not significant).

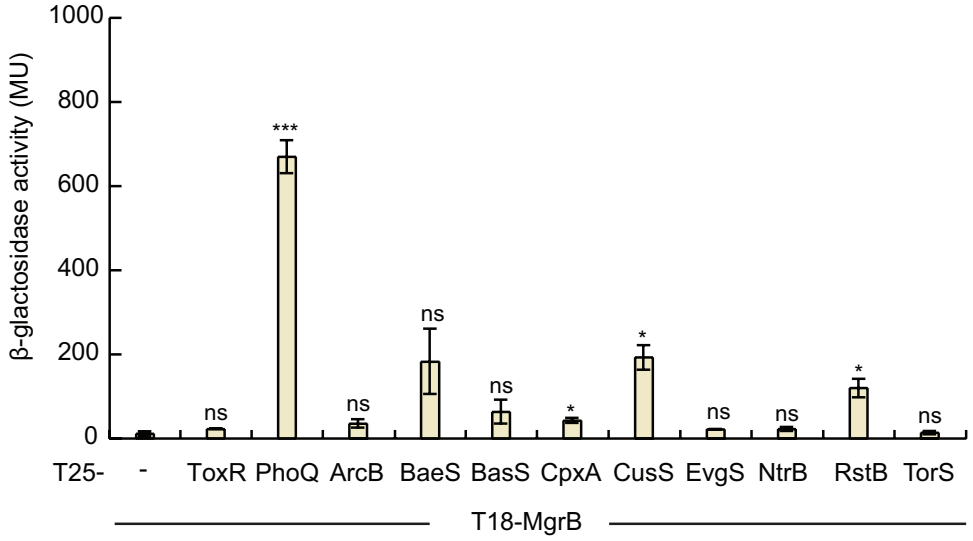

S6 Fig. **MgrB interacts with other histidine kinases in a bacterial two-hybrid assay.** Bacterial two-hybrid (BACTH) assays with cells expressing protein fusions to the T18 and T25 subunits of *B. pertussis* adenylyl cyclase. *β*-gal expression from the *lac* promoter was monitored as a measure of interactions between T18-MgrB and T25 fusion with either ToxR, ArcB, BaeS, CpxA, CusS, EvgS, NtrB, RstB and TorS. The statistical significances of changes in reporter activity were calculated with *t* tests by comparing to the negative control (T18-MgrB/T25 only) and indicated with asterisks (*** $P \leq 0.001$, ** $P \leq 0.01$, * $P \leq 0.05$, ns = not significant).

References

1. Duval M, Cossart P. Small bacterial and phagic proteins: an updated view on a rapidly moving field. Curr Opin Microbiol. 2017;39:81-8. doi: 10.1016/j.mib.2017.09.010. PubMed PMID: 29111488.
2. Storz G, Wolf YI, Ramamurthi KS. Small proteins can no longer be ignored. Annu Rev Biochem. 2014;83:753-77. doi: 10.1146/annurev-biochem-070611-102400. PubMed PMID: 24606146; PubMed Central PMCID: PMCPMC4166647.
3. VanOrsdel CE, Kelly JP, Burke BN, Lein CD, Oufiero CE, Sanchez JF, et al. Identifying New Small Proteins in Escherichia coli. Proteomics. 2018;18(10):e1700064. doi: 10.1002/pmic.201700064. PubMed PMID: 29645342; PubMed Central PMCID: PMCPMC6001520.
4. Weaver J, Mohammad F, Buskirk AR, Storz G. Identifying Small Proteins by Ribosome Profiling with Stalled Initiation Complexes. MBio. 2019;10(2). doi: 10.1128/mBio.02819-18. PubMed PMID: 30837344; PubMed Central PMCID: PMCPMC6401488.
5. Nakahigashi K, Takai Y, Kimura M, Abe N, Nakayashiki T, Shiwa Y, et al. Comprehensive identification of translation start sites by tetracycline-inhibited ribosome

1048 profiling. DNA Res. 2016;23(3):193-201. doi: 10.1093/dnares/dsw008. PubMed PMID:
1049 27013550; PubMed Central PMCID: PMCPMC4909307.
1050 6. Carol Smith JGC, Jing Wang, Keith M. Derbyshire, Todd A. Gray, Joseph T. Wade.
1051 Pervasive translation in Mycobacterium tuberculosis. bioRxiv. 2019. doi:
1052 https://doi.org/10.1101/665208.
1053 7. Sberro H, Fremin BJ, Zlitni S, Edfors F, Greenfield N, Snyder MP, et al. Large-Scale
1054 Analyses of Human Microbiomes Reveal Thousands of Small, Novel Genes. Cell.
1055 2019;178(5):1245-59 e14. doi: 10.1016/j.cell.2019.07.016. PubMed PMID: 31402174.
1056 8. Hemm MR, Paul BJ, Schneider TD, Storz G, Rudd KE. Small membrane proteins
1057 found by comparative genomics and ribosome binding site models. Mol Microbiol.
1058 2008;70(6):1487-501. doi: 10.1111/j.1365-2958.2008.06495.x. PubMed PMID: 19121005;
1059 PubMed Central PMCID: PMCPMC2614699.
1060 9. Stock AM, Robinson VL, Goudreau PN. Two-Component Signal Transduction. Annu
1061 Rev Biochem. 2000;69(1):183-215. doi:
1062 papers2://publication/doi/10.1146/annurev.biochem.69.1.183.
1063 10. Groisman EA. The Pleiotropic Two-Component Regulatory System PhoP-PhoQ. J
1064 Bacteriol. 2001;183(6):1835-42. doi: papers2://publication/doi/10.1128/JB.183.6.1835-
1065 1842.2001.
1066 11. Garcia Vescovi E, Soncini FC, Groisman EA. Mg^{2+} as an extracellular signal:
1067 environmental regulation of *Salmonella* virulence. Cell. 1996;84(1):165-74. PubMed PMID:
1068 8548821.
1069 12. Prost LR, Daley ME, Le Sage V, Bader MW, Le Moual H, Klevit RE, et al.
1070 Activation of the bacterial sensor kinase PhoQ by acidic pH. Mol Cell. 2007;26(2):165-74.
1071 doi: 10.1016/j.molcel.2007.03.008. PubMed PMID: 17466620.
1072 13. Bader MW, Sanowar S, Daley ME, Schneider AR, Cho U, Xu W, et al. Recognition
1073 of antimicrobial peptides by a bacterial sensor kinase. Cell. 2005;122(3):461-72. doi:
1074 10.1016/j.cell.2005.05.030. PubMed PMID: 16096064.
1075 14. Yuan J, Jin F, Glatter T, Sourjik V. Osmosensing by the bacterial PhoQ/PhoP two-
1076 component system. Proc Natl Acad Sci U S A. 2017;114(50):E10792-E8. doi:
1077 10.1073/pnas.1717272114. PubMed PMID: 29183977; PubMed Central PMCID:
1078 PMCPMC5740661.
1079 15. Goulian M. Two-component signaling circuit structure and properties. Curr Opin
1080 Microbiol. 2010;13(2):184-9. doi: papers2://publication/doi/10.1016/j.mib.2010.01.009.
1081 16. Wang H, Yin X, Wu Orr M, Dambach M, Curtis R, Storz G. Increasing intracellular
1082 magnesium levels with the 31-amino acid MgtS protein. Proc Natl Acad Sci U S A.
1083 2017;114(22):5689-94. doi: 10.1073/pnas.1703415114. PubMed PMID: 28512220; PubMed
1084 Central PMCID: PMCPMC5465934.
1085 17. Alix E, Blanc-Potard AB. Peptide-assisted degradation of the Salmonella MgtC
1086 virulence factor. EMBO J. 2008;27(3):546-57. doi: 10.1038/sj.emboj.7601983. PubMed
1087 PMID: 18200043; PubMed Central PMCID: PMCPMC2241655.
1088 18. Lippa AM, Goulian M. Feedback inhibition in the PhoQ/PhoP signaling system by a
1089 membrane peptide. PLoS Genet. 2009;5(12):e1000788. doi: 10.1371/journal.pgen.1000788.
1090 PubMed PMID: 20041203; PubMed Central PMCID: PMCPMC2789325.
1091 19. Salazar ME, Podgornaia AI, Laub MT. The small membrane protein MgrB regulates
1092 PhoQ bifunctionality to control PhoP target gene expression dynamics. Mol Microbiol. 2016.
1093 doi: 10.1111/mmi.13471. PubMed PMID: 27447896.
1094 20. Lippa AM, Goulian M. Perturbation of the oxidizing environment of the periplasm
1095 stimulates the PhoQ/PhoP system in Escherichia coli. J Bacteriol. 2012;194(6):1457-63. doi:
1096 10.1128/JB.06055-11. PubMed PMID: 22267510; PubMed Central PMCID:
1097 PMCPMC3294871.

1098 21. Yadavalli SS, Carey JN, Leibman RS, Chen AI, Stern AM, Roggiani M, et al.
1099 Antimicrobial peptides trigger a division block in Escherichia coli through stimulation of a
1100 signalling system. Nat Commun. 2016;7:12340. doi: 10.1038/ncomms12340. PubMed
1101 PMID: 27471053; PubMed Central PMCID: PMCPMC4974570.
1102 22. Kidd TJ, Mills G, Sa-Pessoa J, Dumigan A, Frank CG, Insua JL, et al. A Klebsiella
1103 pneumoniae antibiotic resistance mechanism that subdues host defences and promotes
1104 virulence. EMBO Mol Med. 2017;9(4):430-47. doi: 10.15252/emmm.201607336. PubMed
1105 PMID: 28202493; PubMed Central PMCID: PMCPMC5376759.
1106 23. Cannatelli A, Giani T, D'Andrea MM, Di Pilato V, Arena F, Conte V, et al. MgrB
1107 inactivation is a common mechanism of colistin resistance in KPC-producing Klebsiella
1108 pneumoniae of clinical origin. Antimicrob Agents Chemother. 2014;58(10):5696-703. doi:
1109 papers2://publication/doi/10.1128/AAC.03110-14.
1110 24. Olaitan AO, Morand S, Rolain JM. Mechanisms of polymyxin resistance: acquired
1111 and intrinsic resistance in bacteria. Front Microbiol. 2014;5:643. Epub 2014/12/17. doi:
1112 10.3389/fmicb.2014.00643. PubMed PMID: 25505462; PubMed Central PMCID:
1113 PMCPMC4244539.
1114 25. Poirel L, Jayol A, Bontron S, Villegas MV, Ozdamar M, Turkoglu S, et al. The mgrB
1115 gene as a key target for acquired resistance to colistin in Klebsiella pneumoniae. J
1116 Antimicrob Chemother. 2015;70(1):75-80. doi: 10.1093/jac/dku323. PubMed PMID:
1117 25190723.
1118 26. Eguchi Y, Itou J, Yamane M, Demizu R, Yamato F, Okada A, et al. B1500, a small
1119 membrane protein, connects the two-component systems EvgS/EvgA and PhoQ/PhoP in
1120 Escherichia coli. Proc Natl Acad Sci USA. 2007;104(47):18712-7. doi:
1121 papers2://publication/doi/10.1073/pnas.0705768104.
1122 27. Eguchi Y, Ishii E, Hata K, Utsumi R. Regulation of acid resistance by connectors of
1123 two-component signal transduction systems in Escherichia coli. J Bacteriol.
1124 2011;193(5):1222-8. doi: 10.1128/JB.01124-10. PubMed PMID: 21193607; PubMed Central
1125 PMCID: PMCPMC3067605.
1126 28. Roggiani M, Yadavalli SS, Goulian M. Natural variation of a sensor kinase
1127 controlling a conserved stress response pathway in Escherichia coli. PLoS Genet.
1128 2017;13(11):e1007101. Epub 2017/11/16. doi: 10.1371/journal.pgen.1007101. PubMed
1129 PMID: 29140975; PubMed Central PMCID: PMCPMC5706723.
1130 29. Burton NA, Johnson MD, Antczak P, Robinson A, Lund PA. Novel aspects of the
1131 acid response network of E. coli K-12 are revealed by a study of transcriptional dynamics.
1132 Journal of Molecular Biology. 2010. doi: papers2://publication/uuid/EE91AF7A-5760-40B4-
1133 B549-BE44E24F43E7.
1134 30. Gerken H, Charlson ES, Cicirelli EM, Kenney LJ, Misra R. MzrA: a novel modulator
1135 of the EnvZ/OmpR two-component regulon. Mol Microbiol. 2009;72(6):1408-22. doi:
1136 papers2://publication/doi/10.1111/j.1365-2958.2009.06728.x.
1137 31. Ishii E, Eguchi Y, Utsumi R. Mechanism of activation of PhoQ/PhoP two-component
1138 signal transduction by SafA, an auxiliary protein of PhoQ histidine kinase in Escherichia coli.
1139 Biosci Biotechnol Biochem. 2013;77(4):814-9. doi:
1140 papers2://publication/doi/10.1271/bbb.120970.
1141 32. Gerken H, Misra R. MzrA-EnvZ interactions in the periplasm influence the
1142 EnvZ/OmpR two-component regulon. J Bacteriol. 2010. doi:
1143 papers2://publication/uuid/0796C281-CF57-426D-AB5B-52D4AAA89C30.
1144 33. Leeds JA, Beckwith J. Lambda repressor N-terminal DNA-binding domain as an
1145 assay for protein transmembrane segment interactions in vivo. J Mol Biol. 1998;280(5):799-
1146 810. Epub 1998/07/22. doi: 10.1006/jmbi.1998.1893. PubMed PMID: 9671551.

1147 34. Eguchi Y, Ishii E, Yamane M, Utsumi R. The connector SafA interacts with the
1148 multi-sensing domain of PhoQ in Escherichia coli. Mol Microbiol. 2012;85(2):299-313. doi:
1149 10.1111/j.1365-2958.2012.08114.x. PubMed PMID: 22651704.
1150 35. Sampson BA, Misra R, Benson SA. Identification and characterization of a new gene
1151 of Escherichia coli K-12 involved in outer membrane permeability. Genetics.
1152 1989;122(3):491-501. PubMed PMID: 2547691; PubMed Central PMCID:
1153 PMCPMC1203724.
1154 36. Battesti A, Bouveret E. The bacterial two-hybrid system based on adenylate cyclase
1155 reconstitution in Escherichia coli. Methods. 2012;58(4):325-34. doi:
1156 papers2://publication/doi/10.1016/j.ymeth.2012.07.018.
1157 37. Karimova G, Pidoux J, Ullmann A, Ladant D. A bacterial two-hybrid system based on
1158 a reconstituted signal transduction pathway. Proc Natl Acad Sci U S A. 1998;95(10):5752-6.
1159 Epub 1998/05/20. PubMed PMID: 9576956; PubMed Central PMCID: PMCPMC20451.
1160 38. Kentner D, Sourjik V. Dynamic map of protein interactions in the Escherichia coli
1161 chemotaxis pathway. Mol Syst Biol. 2009;5:238. doi: 10.1038/msb.2008.77. PubMed PMID:
1162 19156130; PubMed Central PMCID: PMCPMC2644175.
1163 39. Sourjik V, Vaknin A, Shimizu TS, Berg HC. In vivo measurement by FRET of
1164 pathway activity in bacterial chemotaxis. Methods Enzymol. 2007;423:365-91. doi:
1165 10.1016/S0076-6879(07)23017-4. PubMed PMID: 17609141.
1166 40. Meiresonne NY, van der Ploeg R, Hink MA, den Blaauwen T. Activity-Related
1167 Conformational Changes in d,d-Carboxypeptidases Revealed by In Vivo Periplasmic Forster
1168 Resonance Energy Transfer Assay in Escherichia coli. MBio. 2017;8(5). doi:
1169 10.1128/mBio.01089-17. PubMed PMID: 28900026; PubMed Central PMCID:
1170 PMCPMC5596342.
1171 41. Fink A, Sal-Man N, Gerber D, Shai Y. Transmembrane domains interactions within
1172 the membrane milieu: principles, advances and challenges. Biochim Biophys Acta.
1173 2012;1818(4):974-83. Epub 2011/12/14. doi: 10.1016/j.bbamem.2011.11.029. PubMed
1174 PMID: 22155642.
1175 42. von Heijne G. Membrane-protein topology. Nature Reviews Molecular Cell Biology.
1176 2006;7:909. doi: 10.1038/nrm2063
1177 https://www.nature.com/articles/nrm2063 - supplementary-information.
1178 43. Ulmschneider MB, Sansom MS. Amino acid distributions in integral membrane
1179 protein structures. Biochim Biophys Acta. 2001;1512(1):1-14. Epub 2001/05/04. PubMed
1180 PMID: 11334619.
1181 44. Matamouros S, Hager KR, Miller SI. HAMP Domain Rotation and Tilting
1182 Movements Associated with Signal Transduction in the PhoQ Sensor Kinase. MBio.
1183 2015;6(3):e00616-15. doi: 10.1128/mBio.00616-15. PubMed PMID: 26015499; PubMed
1184 Central PMCID: PMCPMC4447245.
1185 45. Yau WM, Wimley WC, Gawrisch K, White SH. The preference of tryptophan for
1186 membrane interfaces. Biochemistry. 1998;37(42):14713-8. doi: 10.1021/bi980809c. PubMed
1187 PMID: 9778346.
1188 46. de Jesus AJ, Allen TW. The role of tryptophan side chains in membrane protein
1189 anchoring and hydrophobic mismatch. Biochim Biophys Acta. 2013;1828(2):864-76. doi:
1190 10.1016/j.bbamem.2012.09.009. PubMed PMID: 22989724.
1191 47. Goldberg SD, Clinthorne GD, Goulian M, DeGrado WF. Transmembrane polar
1192 interactions are required for signaling in the Escherichia coli sensor kinase PhoQ. Proc Natl
1193 Acad Sci U S A. 2010;107(18):8141-6. doi: 10.1073/pnas.1003166107. PubMed PMID:
1194 20404199; PubMed Central PMCID: PMCPMC2889538.
1195 48. Bhate MP, Molnar KS, Goulian M, DeGrado WF. Signal transduction in histidine
1196 kinases: insights from new structures. Structure. 2015;23(6):981-94. Epub 2015/05/20. doi:

1197 10.1016/j.str.2015.04.002. PubMed PMID: 25982528; PubMed Central PMCID:
1198 PMCPMC4456306.
1199 49. Bi S, Jin F, Sourjik V. Inverted signaling by bacterial chemotaxis receptors. Nat
1200 Commun. 2018;9(1):2927. doi: 10.1038/s41467-018-05335-w. PubMed PMID: 30050034;
1201 PubMed Central PMCID: PMCPMC6062612.
1202 50. Olaitan AO, Diene SM, Kempf M, Berrazeg M, Bakour S, Gupta SK, et al.
1203 Worldwide emergence of colistin resistance in Klebsiella pneumoniae from healthy humans
1204 and patients in Lao PDR, Thailand, Israel, Nigeria and France owing to inactivation of the
1205 PhoP/PhoQ regulator mgrB: an epidemiological and molecular study. Int J Antimicrob
1206 Agents. 2014;44(6):500-7. Epub 2014/09/30. doi: 10.1016/j.ijantimicag.2014.07.020.
1207 PubMed PMID: 25264127.
1208 51. Cheng YH, Lin TL, Pan YJ, Wang YP, Lin YT, Wang JT. Colistin resistance
1209 mechanisms in Klebsiella pneumoniae strains from Taiwan. Antimicrob Agents Chemother.
1210 2015;59(5):2909-13. Epub 2015/02/19. doi: 10.1128/AAC.04763-14. PubMed PMID:
1211 25691646; PubMed Central PMCID: PMCPMC4394772.
1212 52. Bakthavatchalam YD, Pragasam AK, Biswas I, Veeraraghavan B. Polymyxin
1213 susceptibility testing, interpretative breakpoints and resistance mechanisms: An update. J
1214 Glob Antimicrob Resist. 2018;12:124-36. Epub 2017/10/01. doi: 10.1016/j.jgar.2017.09.011.
1215 PubMed PMID: 28962863.
1216 53. Nordmann P, Jayol A, Poirel L. A Universal Culture Medium for Screening
1217 Polymyxin-Resistant Gram-Negative Isolates. J Clin Microbiol. 2016;54(5):1395-9. Epub
1218 2016/03/18. doi: 10.1128/JCM.00446-16. PubMed PMID: 26984971; PubMed Central
1219 PMCID: PMCPMC4844728.
1220 54. Bonura C, Giuffre M, Aleo A, Fasciana T, Di Bernardo F, Stampone T, et al. An
1221 Update of the Evolving Epidemic of blaKPC Carrying Klebsiella pneumoniae in Sicily, Italy,
1222 2014: Emergence of Multiple Non-ST258 Clones. PLoS One. 2015;10(7):e0132936. Epub
1223 2015/07/16. doi: 10.1371/journal.pone.0132936. PubMed PMID: 26177547; PubMed Central
1224 PMCID: PMCPMC4503429.
1225 55. Haeili M, Javani A, Moradi J, Jafari Z, Feizabadi MM, Babaei E. MgrB Alterations
1226 Mediate Colistin Resistance in Klebsiella pneumoniae Isolates from Iran. Front Microbiol.
1227 2017;8:2470. Epub 2018/01/13. doi: 10.3389/fmicb.2017.02470. PubMed PMID: 29326662;
1228 PubMed Central PMCID: PMCPMC5741654.
1229 56. Baba T, Ara T, Hasegawa M, Takai Y, Okumura Y, Baba M, et al. Construction of
1230 Escherichia coli K-12 in-frame, single-gene knockout mutants: the Keio collection. Mol Syst
1231 Biol. 2006;2:2006 0008. doi: 10.1038/msb4100050. PubMed PMID: 16738554; PubMed
1232 Central PMCID: PMC1681482.
1233 57. Datsenko KA, Wanner BL. One-step inactivation of chromosomal genes in
1234 Escherichia coli K-12 using PCR products. Proc Natl Acad Sci USA. 2000;97(12):6640-5.
1235 doi: papers2://publication/doi/10.1073/pnas.120163297.
1236 58. Ochman H, Ajioka JW, Garza D, Hartl DL. Inverse polymerase chain reaction.
1237 Biotechnology (N Y). 1990;8(8):759-60. Epub 1990/08/01. PubMed PMID: 1366903.
1238 59. Gibson DG, Young L, Chuang RY, Venter JC, Hutchison CA, 3rd, Smith HO.
1239 Enzymatic assembly of DNA molecules up to several hundred kilobases. Nat Methods.
1240 2009;6(5):343-5. Epub 2009/04/14. doi: 10.1038/nmeth.1318. PubMed PMID: 19363495.
1241 60. Besharova O, Suchanek VM, Hartmann R, Drescher K, Sourjik V. Diversification of
1242 Gene Expression during Formation of Static Submerged Biofilms by Escherichia coli. Front
1243 Microbiol. 2016;7:1568. doi: 10.3389/fmicb.2016.01568. PubMed PMID: 27761132;
1244 PubMed Central PMCID: PMCPMC5050211.
1245 61. Miller JH. A Short Course in Bacterial Genetics: CSHL Press; 1992.

1246 62. Thibodeau SA, Fang R, Joung JK. High-throughput beta-galactosidase assay for
1247 bacterial cell-based reporter systems. Biotechniques. 2004;36(3):410-5. doi:
1248 10.2144/04363BM07. PubMed PMID: 15038156.
1249 63. Miyashiro T, Goulian M. Stimulus-dependent differential regulation in the
1250 Escherichia coli PhoQ PhoP system. Proc Natl Acad Sci USA. 2007;104(41):16305-10. doi:
1251 papers2://publication/doi/10.1073/pnas.0700025104.
1252 64. Haldimann A, Wanner BL. Conditional-replication, integration, excision, and
1253 retrieval plasmid-host systems for gene structure-function studies of bacteria. J Bacteriol.
1254 2001;183(21):6384-93. Epub 2001/10/10. doi: 10.1128/JB.183.21.6384-6393.2001. PubMed
1255 PMID: 11591683; PubMed Central PMCID: PMCPMC100134.
1256 65. Bullock WO, Fernandez JM, Short JM. XL1-Blue: a high efficiency plasmid
1257 transforming recA *Escherichia coli* strain with beta-galactosidase selection. BioTechniques.
1258 1987;5:376-9.
1259 66. Cherepanov PP, Wackernagel W. Gene disruption in Escherichia coli: Tc R and Km
1260 R cassettes with the option of Flp-catalyzed excision of the antibiotic-resistance determinant.
1261 Gene. 1995. doi: papers2://publication/uuid/31A60367-CF87-4BF6-B690-93462755E5ED.
1262 67. Hay AJ, Yang M, Xia X, Liu Z, Hammons J, Fenical W, et al. Calcium Enhances Bile
1263 Salt-Dependent Virulence Activation in Vibrio cholerae. Infect Immun. 2017;85(1). Epub
1264 2016/11/17. doi: 10.1128/IAI.00707-16. PubMed PMID: 27849180; PubMed Central
1265 PMCID: PMCPMC5203667.
1266 68. Amann E, Ochs B, Abel KJ. Tightly regulated tac promoter vectors useful for the
1267 expression of unfused and fused proteins in Escherichia coli. Gene. 1988;69(2):301-15.
1268 PubMed PMID: 3069586.
1269

F	sequencing failed
NS	nonsense mutation
FS	frameshift
S	silent mutation
IS	insertion
D	deletion

Label Numbe	Sample Name	Primer Name	sequencing results
90073451	RMphoQ001	pBADfw	**F**
90073452	RMphoQ002	pBADfw	**NS**
90073453	RMphoQ003	pBADfw	**F**
90073454	RMphoQ004	pBADfw	**NS**
90073455	RMphoQ005	pBADfw	**F**
90073456	RMphoQ006	pBADfw	**NS**
90073457	RMphoQ007	pBADfw	**R219G**
90073458	RMphoQ008	pBADfw	**F**
90073459	RMphoQ009	pBADfw	**F**
90073460	RMphoQ010	pBADfw	**R262H**
90073461	RMphoQ011	pBADfw	**F**
90073462	RMphoQ012	pBADfw	**NS**
90073463	RMphoQ013	pBADfw	**F**
90073464	RMphoQ014	pBADfw	**NS**
90073465	RMphoQ015	pBADfw	**F**
90073466	RMphoQ016	pBADfw	**F**
90073467	RMphoQ017	pBADfw	**F**
90073468	RMphoQ018	pBADfw	**F**
90073469	RMphoQ019	pBADfw	**F**
90073470	RMphoQ020	pBADfw	**F**

Label Numbe	Sample Name	Primer Name	sequencing results
90073499	RMphoQ2_001	pBADfw	**NS**
90073500	RMphoQ2_002	pBADfw	**I196F, S217N**
90073501	RMphoQ2_003	pBADfw	**IS**
90073502	RMphoQ2_004	pBADfw	**R262S**
90073503	RMphoQ2_005	pBADfw	**L250M**
90073504	RMphoQ2_006	pBADfw	**WT**
90073505	RMphoQ2_007	pBADfw	**F**
90073506	RMphoQ2_008	pBADfw	**WT**
90073507	RMphoQ2_009	pBADfw	**WT**
90073508	RMphoQ2_010	pBADfw	**F**
90073509	RMphoQ2_011	pBADfw	**WT**
90073510	RMphoQ2_012	pBADfw	**F**
90073511	RMphoQ2_013	pBADfw	**L199H, E237V, S249R**
90073512	RMphoQ2_014	pBADfw	**W211C, L247Q**
90073513	RMphoQ2_015	pBADfw	**W215L**
90073514	RMphoQ2_016	pBADfw	**D**
90073515	RMphoQ2_017	pBADfw	**R262L**
90073516	RMphoQ2_018	pBADfw	**F**
90073517	RMphoQ2_019	pBADfw	**FS**
90073518	RMphoQ2_020	pBADfw	**FS**

90073471	RMphoQ021	pBADfw	**F**	90073519	RMphoQ2_021	pBADfw	**F**
90073472	RMphoQ022	pBADfw	**F**	90073520	RMphoQ2_022	pBADfw	**F**
90073473	RMphoQ023	pBADfw	**R219G**	90073521	RMphoQ2_023	pBADfw	**A213T**
90073474	RMphoQ024	pBADfw	**F**	90073522	RMphoQ2_024	pBADfw	**D**
90073475	RMphoQ025	pBADfw	**K259R**	90073523	RMphoQ2_025	pBADfw	**WT**
90073476	RMphoQ026	pBADfw	**N235Z**	90073524	RMphoQ2_026	pBADfw	**F**
90073477	RMphoQ027	pBADfw	**WT**	90073525	RMphoQ2_027	pBADfw	**F**
90073478	RMphoQ028	pBADfw	**WT**	90073526	RMphoQ2_028	pBADfw	**FS**
90073479	RMphoQ029	pBADfw	**WT**	90073527	RMphoQ2_029	pBADfw	**F**
90073480	RMphoQ030	pBADfw	**WT**	90073528	RMphoQ2_030	pBADfw	**WT**
90073481	RMphoQ031	pBADfw	**V198A, R219C**	90073529	RMphoQ2_031	pBADfw	**FS**
90073482	RMphoQ032	pBADfw	**WT**	90073530	RMphoQ2_032	pBADfw	**NS**
90073483	RMphoQ033	pBADfw	**WT**	90073531	RMphoQ2_033	pBADfw	**WT**
90073484	RMphoQ034	pBADfw	**S**	90073532	RMphoQ2_034	pBADfw	**WT**
90073485	RMphoQ035	pBADfw	**WT**	90073533	RMphoQ2_035	pBADfw	**F**
90073486	RMphoQ036	pBADfw	**WT**	90073534	RMphoQ2_036	pBADfw	**L247Q mixed with WT**
90073487	RMphoQ037	pBADfw	**WT**	90073535	RMphoQ2_037	pBADfw	**WT**
90073488	RMphoQ038	pBADfw	**V198E, E230L**	90073536	RMphoQ2_038	pBADfw	**WT**
90073489	RMphoQ039	pBADfw	**WT**	90073537	RMphoQ2_039	pBADfw	**WT**
90073490	RMphoQ040	pBADfw	**WT**	90073538	RMphoQ2_040	pBADfw	**WT**
90073491	RMphoQ041	pBADfw	**WT**	90073539	RMphoQ2_041	pBADfw	**WT**
90073492	RMphoQ042	pBADfw	**V198A, R219C**	90073540	RMphoQ2_042	pBADfw	**FS**

Label Numbe	Sample Name	Primer Name	sequencing results
90073546	RMphoQ3_001	pBADfw	**F**
90073547	RMphoQ3_002	pBADfw	**I221T**
90073548	RMphoQ3_003	pBADfw	**NS**
90073549	RMphoQ3_004	pBADfw	**R262C**
90073550	RMphoQ3_005	pBADfw	**WT**
90073551	RMphoQ3_006	pBADfw	**V251I**
90073552	RMphoQ3_007	pBADfw	**FS**
90073553	RMphoQ3_008	pBADfw	**S217C**
90073554	RMphoQ3_009	pBADfw	**WT**
90073555	RMphoQ3_010	pBADfw	**A223T**
90073556	RMphoQ3_011	pBADfw	**D274N**
90073557	RMphoQ3_012	pBADfw	**FS**
90073558	RMphoQ3_013	pBADfw	**FS**
90073559	RMphoQ3_014	pBADfw	**WT**
90073560	RMphoQ3_015	pBADfw	**FS**
90073561	RMphoQ3_016	pBADfw	**W211R**
90073562	RMphoQ3_017	pBADfw	**L210M**
90073563	RMphoQ3_018	pBADfw	**WT**
90073564	RMphoQ3_019	pBADfw	**FS**
90073565	RMphoQ3_020	pBADfw	**D274N**
90073566	RMphoQ3_021	pBADfw	**S217C**
90073567	RMphoQ3_022	pBADfw	**V206N**
90073568	RMphoQ3_023	pBADfw	**T270R**
90073569	RMphoQ3_024	pBADfw	**L203Q**
90073570	RMphoQ3_025	pBADfw	**FS**
90073571	RMphoQ3_026	pBADfw	**F**
90073572	RMphoQ3_027	pBADfw	**L209P**

Label Numbe	Sample Name	Primer Name	sequencing results
90073573	RMphoQ3_028	pBADfw	**WT**
90073574	RMphoQ3_029	pBADfw	**WT**
90073575	RMphoQ3_030	pBADfw	**NS**
90073576	RMphoQ3_031	pBADfw	**R256L**
90073577	RMphoQ3_032	pBADfw	**W216R, E230D**
90073578	RMphoQ3_033	pBADfw	**IS**
90073579	RMphoQ3_034	pBADfw	**WT**
90073580	RMphoQ3_035	pBADfw	**F**
90073581	RMphoQ3_036	pBADfw	**F**
90073582	RMphoQ3_037	pBADfw	**IS**
90073583	RMphoQ3_038	pBADfw	**A201S**

Label Numbe	Sample Name	Primer Name	sequencing results
90073594	RMphoQ4_001	pBADfw	**FS**
90073595	RMphoQ4_002	pBADfw	**A214T**
90073596	RMphoQ4_003	pBADfw	**FS**
90073597	RMphoQ4_004	pBADfw	**FS**
90073598	RMphoQ4_005	pBADfw	**L254R**
90073599	RMphoQ4_006	pBADfw	**FS**
90073600	RMphoQ4_007	pBADfw	**F195L**
90073601	RMphoQ4_008	pBADfw	**FS**
90073602	RMphoQ4_009	pBADfw	**IS**
90073603	RMphoQ4_010	pBADfw	**WT**
90073604	RMphoQ4_011	pBADfw	**FS**
90073605	RMphoQ4_012	pBADfw	**IS**
90073606	RMphoQ4_013	pBADfw	**F195L**